

MOL #67959

Functional and Biochemical Properties of RyR1 Channels from Heterozygous R163C Malignant Hyperthermia Susceptible Mice

Wei Feng^{*}, Genaro C. Barrientos^{*}, Gennady Cherednichenko, Tianzhong Yang, Isela T. Padilla, Kim Truong, Paul D. Allen, José R. Lopez and Isaac N. Pessah

Department of Molecular Biosciences, School of Veterinary Medicine, University of California, Davis, CA (WF, GCB, GC, ITP, KT, INP); Department of Anesthesia, Perioperative and Pain Medicine, Brigham and Women's Hospital, Boston, MA (TY, JRL, PDA)

MOL #67959

Running Title: Basal RyR1 channel dysfunction in heterozygous R163C MH mice

Correspondence: Isaac N. Pessah, Department of Molecular Biosciences, School of Veterinary Medicine, One Shields Avenue, University of California, Davis, CA 95616, inpessah@ucdavis.edu

Number of text pages:	26
Tables:	0
Figures:	9
References:	42
Words in Abstract:	250
Words in Introduction:	702
Words in Discussion:	1,605

ABBREVIATIONS:

BLM, bilayer lipid membrane; BTS, *N*-benzyl-*p*-toluene sulphonamide ; $[Ca^{2+}]_{rest}$, cellular cytoplasmic resting Ca^{2+} ; ER, endoplasmic reticulum; EC, excitation-contraction; ECCE, excitation-coupled calcium entry; EGTA, ethylene glycol-bis(2-aminoethylether)-*N,N,N',N'*-tetraacetic acid; FDB, flexor digitorum brevis; FKBP12, FK506 binding protein 12 kilodalton; HEPES, (4-(2-hydroxyethyl)-1-piperazineethanesulfonic acid); MH, malignant hyperthermia; MHS, malignant hyperthermia susceptibility; P_o , open probability; RyR1, ryanodine receptor type 1; SERCA, SR/ER Calcium ATPase; SR, sarcoplasmic reticulum; SOCE, store operated calcium entry; τ_c , mean closed-dwell time; τ_o , mean open-dwell time; TG, thapsigargin.

MOL #67959

Abstract

Mutations in ryanodine receptor type 1 (RyR1) confer malignant hyperthermia susceptibility (MHS). How inherent impairments in Ca^{2+} channel regulation impact skeletal muscle function in myotubes and adult fibers under basal (non-triggering) conditions are not understood. Myotubes, adult FDB fibers, and SR skeletal membranes were isolated from heterozygous knock-in R163C and wild type (WT) mice. Compared to WT, R163C myotubes have reduced Ca^{2+} transient amplitudes in response to electrical field pulses, however R163C FDB fibers do not differ in their responses to electrical stimuli, despite heightened $[\text{Ca}^{2+}]_{\text{rest}}$ and sensitivity to halothane. Immunoblotting of membranes from each genotype shows similar expression of RyR1, FKPB12 and Ca^{2+} -ATPase, but RyR1²⁸⁴⁴Ser phosphorylation in R163C muscle is 31% higher than WT ($p < 0.001$). RyR1 channels reconstituted in planar lipid bilayers (BLM) reveal ~65% of R163C channels exhibit ≥ 2 -fold greater open probability (P_o) than WT, with prolonged mean open-dwell times and shortened closed-dwell times. [³H]Ry binding and single channel analyses show that R163C-RyR1 has altered regulation compared to WT: (1) 3-Fold higher sensitivity to Ca^{2+} activation; (2) 2-Fold greater [³H]Ry receptor occupancy; (3) comparatively higher channel activity, even in reducing glutathione buffer; (4) enhanced RyR1 activity both at 25 and 37°C; (5) Elevated cytoplasmic $[\text{Ca}^{2+}]_{\text{rest}}$. R163C channels are inherently more active than WT, a functional impairment that cannot be reversed by dephosphorylation with protein phosphatase. Dysregulated R163C channels produce a more overt phenotype in myotubes than in adult fibers in the absence of triggering agents, suggesting tighter negative regulation of R163C-RyR1 within the CRU of adult fibers.

MOL #67959

Introduction

Human malignant hyperthermia (MH) susceptible patients remain subclinical until challenged with one or more pharmacologic triggering agents, including halogenated volatile anesthetics and depolarizing neuromuscular blockers (Zhou, 2010). A fulminant MH episode during the perioperative period is often lethal if not promptly treated with dantrolene. When a familial history of MH is suspected (Lehmann-Horn et al., 2008), MH susceptibility (MHS) is typically diagnosed with an *in vitro* contracture test (IVCT). Although IVCT testing is a good prognosticator of MH, fatal cases continue to occur annually in the US and throughout the world (Zhou, 2010). MHS is an inherited autosomal dominant muscle disorder with a heterogeneous etiology. Common to all fulminant MH episodes is a severe defect in skeletal muscle Ca^{2+} regulation that is not evident (remains subclinical) in the absence of an environmental trigger. More than 50% of the families with a familial history of MHS have linkage to one of >175 mutations within RYR1 located on 19q13.1, the gene that encodes the skeletal isoform of ryanodine receptor type 1 (RyR1) (Robinson et al., 2006). RyR1 is responsible for releasing ionized calcium (Ca^{2+}) from SR stores during excitation-contraction (EC) coupling, and is essential for muscle contraction (Takeshima et al., 1994; Buck et al 1997). Of the additional loci linked to MHS, one within the CACNA1S gene that encodes for the pore forming subunit of the L-type voltage-dependent Ca^{2+} channel $\text{Ca}_v1.1$ localized within t-tubule membranes (also termed DHPR) (Robinson et al., 2003) that is responsible for RyR1 activation during excitation-contraction (EC) coupling leading to muscle contraction. RyR1 and its protein-binding partners assemble a tightly regulated macromolecular complex within the T-tubule-SR junctions termed “ Ca^{2+} release units” (CRUs). A prominent feature of the CRU is a physical

MOL #67959

interaction between the DHPR and RyR1 that permits precise alignment of DHPR tetrads over every other RyR1 (Protasi, 2002), an arrangement that is essential for engaging bidirectional signaling between the DHPR and RyR1. Thus the ultrastructural organization of the CRU proteins is tightly linked to precise positive and negative regulation between DHPR and RyR1 Ca^{2+} channels (Sheridan et al., 2006).

Recent studies have shown that MHS mutations alter bidirectional signaling between DHPR and RyR1 even in the absence of triggering agents (Bannister et al., 2010b). Thus Ca^{2+} dysregulation in skeletal muscle does not only manifest during the acute period of a triggered MH episode. Chronic elevation of Ca^{2+} in the myoplasm of resting muscle cells ($[\text{Ca}^{2+}]_{\text{rest}}$) is a common feature of skeletal muscle expressing MHS mutations (Yang et al., 2007a). In this respect, expression of normal RyR1 channels appears to critically regulate $[\text{Ca}^{2+}]_{\text{rest}}$ in skeletal myotubes by contributing Ca^{2+} leak from SR and causing increased Ca^{2+} entry (Eltit et al., 2010). Thus altered DHPR-RyR1 bidirectional signaling and elevated $[\text{Ca}^{2+}]_{\text{rest}}$ may confer MHS.

Heterozygosis for R163C-RyR1 (R163C) is one of the five most common mutations conferring MHS in humans (Robinson et al., 2006). A knock-in mouse model of R163C was generated and shown to possess the hallmarks of MHS (Yang et al., 2006). Although R163C homozygous mice are not viable at birth, mice heterozygous for the mutation (referred to as R163C mice throughout the manuscript) model the human condition in that they exhibit no overt clinical phenotype until they are challenged with either heat stress or a general anesthetic (e.g., halothane), which triggers a fulminant MH episode. Myotubes isolated from R163C MHS mice also show significant deviations from WT myotubes in the absence of triggering agents, including: (1) elevated $[\text{Ca}^{2+}]_{\text{rest}}$ (Yang et al., 2007b), (2)

MOL #67959

enhanced excitation-coupled Ca^{2+} entry (ECCE) (Cherednichenko et al., 2008), (3) altered retrograde signaling to the DHPR resulting in a shift of SR Ca^{2+} release to more hyperpolarized potentials and a concomitant decrease in the transient amplitude ($\Delta F/F_0$) (Bannister et al., 2010a), and (4) higher sensitivity of R163C expressing myotubes to stimulation by pharmacological and physiological ligands such as caffeine, 4-chloro-*m*-cresol and K^+ -induced depolarization than WT (Esteve et al., 2010b). The present study identifies fundamental biochemical and functional impairments inherent in R163C channels isolated from R163C heterozygous mice. Dysregulated R163C channels produce a more overt phenotype in cultured myotubes than in adult fibers in the absence of a triggering agent, providing the first evidence of tighter negative regulation of R163C in adult fibers, possibly conferred by DHPR.

Methods

Animal use

All collection of mouse tissues was conducted using protocols approved by the Institutional Animal Care and Use Committees at the University of California at Davis and Department of Anesthesia, Perioperative and Pain Medicine, Brigham and Women's Hospital.

Preparation of primary myotubes and adult FDB fibers

Primary skeletal myoblast lines were isolated from 1- to 2-day old C57/B6 wild type (WT) mice and from newborn mice heterozygous for mutation R163C MH as previously described (Cherednichenko et al., 2004). The myoblasts were expanded in 10 cm cell-culture treated Corning dishes coated with collagen (Calbiochem, Richmond, CA) and

MOL #67959

were plated onto 96-well μ -clear plates (Greiner) coated with MATRIGEL (Becton Dickinson) for Ca^{2+} imaging studies. Upon reaching ~80% confluence, growth factors were withdrawn and the cells allowed to differentiate into myotubes over a period of 3 days.

Flexor digitorum brevis (FDB) were dissected from 3-6 month-old WT and R163C heterozygous mice and single intact myofibers enzymatically isolated as described previously (Brown et al., 2007). In order to reduce stress-activated SR Ca^{2+} release during isolation, especially in R163C fibers, 10 μM dantrolene was included in the initial dissociation medium. After isolation, the fibers were plated on MATRIGEL-coated plates (BD Biosciences, San Jose, CA) and maintained in Dulbecco's modified Eagle's medium (Invitrogen, Carlsbad, CA) supplemented with 10% fetal bovine serum (Thermo Scientific) and 0.1 mg/ml penicillin–streptomycin (Sigma) in the absence of dantrolene. Fibers were kept overnight in a 5% CO_2 incubator, and experiments were conducted within 12 to 24 h after plating.

Measurements of Ca^{2+} transients

Myotubes were loaded with the Ca^{2+} indicator fluo-4-AM (Molecular Probes, Eugene, OR) at 37°C for 20 min in imaging buffer composed of (in mM) 125 NaCl, 5 KCl, 2 CaCl_2 , 1.2 MgSO_4 , 6 dextrose, and 25 HEPES, pH 7.4 supplemented with 0.05% bovine serum albumin). Myotubes were then washed 3 times with imaging buffer and transferred to the stage of a Nikon Diaphot inverted microscope and illuminated at the isosbestic wavelength for fura-2 or 494 nm for fluo-4 with a DeltaRam excitation source (Photon Technology International; PTI, Lawrenceville, NJ). Fluorescence emission at 510nm was captured from regions of interest within each myotube from 3-10 individual cells at 6 frames per second using a Nikon 40x na 1.3 objective, IC-300 ICCD camera and digitized and analyzed with

MOL #67959

ImageMaster software (PTI). Electrical field stimuli were applied using two platinum electrodes fixed to opposite sides of the well and connected to an AMPI Master 8 stimulator set at 7-V, 0.5 ms bipolar total pulse duration, over a range of frequencies (2-60 Hz, 10 sec pulse train duration, 30 sec rest between pulse trains). Transient amplitude was measured by normalizing peak change in fluo-4 fluorescence (ΔF) to the fluorescence baseline (F_0) and presented as mean $\Delta F/F_0$ for each myotube included in the analysis. The mean \pm SEM was calculated from the number of cells indicated in the figure legends, which were obtained from at least two different experimental days. Statistical analysis was performed with one-way ANOVA.

FDBs fibers were loaded with Fluo-4 AM (10 μ M; 40 min at RT) in normal Ringer's solution containing (in mM) 146 NaCl, 4.7 KCl, 0.6 MgSO₄, 6 glucose, 25 HEPES, 2 CaCl₂ and 0.02% pluronic127 (Invitrogen). The cells were then washed three times with Ringer's and transferred to the stage of an IX71 inverted microscope equipped with a 40x 0.9 na objective (Olympus, Center Valley, PA) and illuminated 494 nm to excite Fluo-4 with a DeltaRam wavelength selectable light source. The contractility inhibitor BTS (*N*-benzyl-*p*-toluene sulphonamide; 20 μ M) was added to the imaging buffer prior to initiating measurement to prevent movement artifacts. Fluorescence emission at 510 nm was captured from individual fibers. Electrical field stimuli were applied using two platinum electrodes fixed to opposite sides of the well and connected to an A.M.P.I. Master 8 stimulator set at 4-V, 0.5-ms bipolar pulse duration over a range of frequencies (1-20 Hz; 10-s pulse train duration). Halothane was dissolved in Ringer's solution and the concentration was confirmed by mass spectrometry. The FDB fibers were perfused with 0.1% halothane prepared just before needed. Fluo-4 fluorescence emission was measured

MOL #67959

at 30 frames per sec using Cascade 512B camera (Photometrics, Tucson, AZ). The images were acquired using the Easy Ratio Pro software (PTI). The data were analyzed using Origin 7 software (OriginLab Corporation MA). Transients were normalized to the fluorescence baseline (F_0) of each individual fiber and the mean integrated area within the evoked responses calculated from the number of fibers indicated in the figure legend. Statistical comparisons were performed with an unpaired Student's t-test.

Determination of $[Ca^{2+}]_{rest}$

Ca^{2+} selective microelectrodes. Double-barreled Ca^{2+} -selective microelectrodes were prepared and calibrated as previously described (Eltit et al., 2010). Only those electrodes with a linear relationship between pCa3 and pCa8 (Nernstian response, 28.5 mV per pCa unit at 24°C) were used experimentally. To better mimic the intracellular ionic conditions all calibration solutions were supplemented with 1mM Mg^{2+} . All electrodes were then re-calibrated after making measurements of $[Ca^{2+}]_{rest}$ and if the two calibration curves did not agree within 3mV from pCa 7 to pCa 8, the data from that microelectrode was discarded.

Recording of V_m and $[Ca^{2+}]_{rest}$. Measurements were performed on two preparations; cultured myotubes and mice sedated with non-triggering ketamine/xylazine (100/5 mg/kg). Once mice were fully anesthetized (lack of tail pinch response), small incisions were made to expose the vastus lateralis muscle of each leg and the fibers were impaled with the double-barreled microelectrode. Potentials were recorded via high impedance amplifier (WPI FD-223, Sarasota, FL). The potential from the 3M KCl barrel (V_m) was subtracted electronically from V_{CaE} , to produce a differential Ca^{2+} -specific potential (V_{Ca}) that represents the $[Ca^{2+}]_{rest}$. V_m and V_{Ca} were filtered (30-50 KHz) to improve the signal-to-noise ratio and stored in a computer for further analysis.

MOL #67959

Isolation of membrane fractions from mouse skeletal muscle

Skeletal muscles collected from either WT or heterozygous R163C knock-in mice (1-3 animals per preparation, 3-6 months of age) were minced on ice, placed in ice-cold buffer containing (in mM) sucrose (300), imidazole (5), PMSF (0.01), and leupeptin (5 μ g/ml), pH 7.4, and homogenized with 3 sequential bursts (30s each) of a PowerGen 700D (Fisher, Pittsburgh, Pennsylvania), at 9,000, 18,000 and 18,000 rpm. Homogenates were centrifuged at 10,000g for 20 min. Supernatants were saved, the pellets subjected to a second round of homogenization, and centrifugation at the same settings described above. The remaining pellets were discarded, the supernatants combined and poured through 4-layers of cheesecloth. The filtrate was centrifuged at 110,000g for 60min at 4°C. Pellets were resuspended in sucrose (300), Hepes (10), pH 7.4, aliquoted into microfuge tubes (100 μ l/sample), and either stored at -80°C for biochemical analyses, or subjected to further purification to obtain membranes enriched in junctional SR (JSR). Protein concentration for each preparation was determined using the DC Protein Assay kit (Bio-Rad, Hercules, CA).

Western blotting

Skeletal muscle membrane preparations were denatured in SDS-PAGE sample buffer (Bio Rad, Hercules CA) containing 2.5% 2-mercaptoethanol at 60° C for 5 min. Protein (10 or 15 μ g/lane) was loaded onto Tris- acetate 4-12% or 4-20% acrylamide gradient SDS-PAGE gels (Invitrogen), electrophoresed at 150V for 75 min (4°C), transferred to PVDF membranes at 30V for 15hr and then at 110V for another 1 hour (4°C). Membranes were blocked with Odyssey Blocking Buffer (LI-COR, NE) for 30 minute and incubated overnight at 4°C with the primary antibodies. Total RyR1 was detected with antibody 34C (Airey et al., 1990) at 1:1000 dilution (Developmental Studies Hybridoma Bank University of Iowa,

MOL #67959

Iowa City). Phospho-epitope-specific antibody that recognizes mouse RyR1²⁸⁴⁴Ser, a PKA-phosphorylation site (Reiken et al., 2003), was purchased from Abcam (ab59225) and used at 1:2,000 dilution. SR/ER Ca²⁺-ATPase was detected using a SERCA1 selective monoclonal (Thermo Scientific Pierce MA3-911) diluted to 1:5000 or 1:20,000. FKBP12 was detected using a commercial polyclonal antibody (Pierce Cat# PA1-026A) diluted 1:2500. After incubation with primary antibody, each PVDF membrane was washed 5 times, 5 minutes each, with PBS containing 0.1 % Tween-20 and incubated with infrared fluorescent conjugated secondary antibodies diluted to 1:10,000; 800 nm fluorescent conjugated goat anti-mouse (LI-COR, 926-32210) and 700 nm fluorescent conjugated goat anti-rabbit (LI-COR, 926-32221). The membranes were washed 5 times with 0.1% Tween-20/PBS and scanned with a LI-COR Odyssey infrared imager and band intensity analyzed using Odyssey version 3.0 software. Signals from each western blot were analyzed for (1) total R163C protein (green channel) normalized to the WT-RyR1 signal on the same blot (each run in duplicate lanes), and (2) the ratio of the phospho-²⁸⁴⁴Ser signal (red channel) to its respective green channel. A total of n=29 separate blots from 5 paired R163C and WT skeletal muscle preparations were analyzed. FKBP12 expression was analyzed from n=2 paired R163C and WT preparations, total blots n=10 from R163C, n=8 from WT. SERCA expression was analyzed from a total of n=3 paired R163C and WT preparations each run in duplicate lanes and normalized to the WT signal.

Dephosphorylation of R163C-RyR1 and WT RyR1 by protein phosphatase 1

Protein phosphatase 1 (PP1; New England BioLabs) was utilized to dephosphorylate SR protein according to the vendor's instructions. The reaction mixture contained 50mM HEPES, 100mM NaCl, 2mM DTT, 1mM MnCl₂, 0.01% Brij 35, pH 7.5, 4mg/ml of SR

MOL #67959

protein (R163C or WT) and 200units/ml PP1, which was incubated at 30°C for 10 min. Then the samples were diluted into SDS-PAGE sample buffer for western blotting or into [³H]ryanodine binding buffer (see below).

Measurements of [³H]ryanodine binding to RyR1

The apparent association or equilibrium binding of [³H]ryanodine ([³H]Ry) to RyR1 were measured at 25°C or 37°C for 0-3 hr with constant shaking in buffer consisting of 100-150 µg protein/ml, 2-5 nM [³H]Ry (PerkinElmer Life and Analytical Sciences, Inc., Wellesley, MA), 250 mM KCl, 20 mM HEPES. RyR1 channel modulators Ca²⁺, Mg²⁺, and/or glutathione were titrated in specific experiments as described in the figure legends. Nonspecific [³H]Ry binding was determined in the presence of 1,000-fold excess unlabeled ryanodine. Bound and free ligand were separated by rapid filtration through Whatman GF/B glass fiber filters using a Brandel cell harvester (Whatman, Gaithersburg, MD) with 5 ml ice-cold buffer (250 mM KCl, 20 mM HEPES, 15 mM NaCl, and 50 µM Ca²⁺, pH 7.4). [³H]Ry retained in filters were quantified by liquid scintillation spectrometry using a scintillation counter (Beckman model 6500). Each experiment was performed on at least 3 independent skeletal muscle preparations, each in triplicate. Linear or non-linear curve-fitting was performed using Origin[®] software (Northampton, MA).

Measurement of SERCA activity

Activity of the thapsigargin-sensitive Ca²⁺-ATPase (SERCA1) was measured in the same skeletal membrane preparations used for western blotting and receptor binding analyses using a coupled enzyme assay that monitors the rate of oxidation of NADH at 340 nm as described previously (Ta et al., 2006). In brief, 1.5ml assay buffer consisted of (mM) 7 HEPES, pH 7.0, 143 KCl, 7 MgCl₂, 0.085 EGTA, 0.43 sucrose, 0.0028

MOL #67959

phosphoenolpyruvate, 1 Na₂ATP, coupling enzyme mixture (700 units of pyruvate kinase II and 1000 units of lactate dehydrogenase), 0.048 free Ca²⁺, and 50 µg/ml of protein at 37°C. Thapsigargin (TG, 0.2 µM) was added to inhibit the SERCA1 component of ATPase activity (negative control). NADH (0.4 mM) was added to initiate measurement of Ca²⁺ (Mg²⁺) ATPase activity. A total of six measurements were made from at least two paired R163C and WT preparations.

Glutathione Stock Solutions and redox potential calculations

GSH was dissolved in degassed 10 mM Hepes buffer, and the solution was adjusted to pH 7.0. Aliquots (~0.5 ml) were transferred to vials and sealed after blowing with argon. The vials were stored at -20 °C for less than a month. Once thawed and opened for use, the vial was discarded. GSSG solution was also made and stored in a similar manner except without degassing and argon protection. Redox potentials were calculated according to the Nernst equation $\{E_h = E_o + RT/2F \ln [(GSSG)/(GSH)^2]\}$, where E_o was the standard state redox potential of glutathione as -240 mV (Hwang et al., 1995).

Single channel measurements in BLM

Planar lipid bilayer was formed by phosphatidylethanolamine/ phosphatidylserine/phosphatidylcholine, 5:3:2 (w/w) (Avanti Polar Lipids, Inc., Alabaster, AL). Chambers defined as *cis* and *trans* contained a 10-fold Cs⁺ gradient (500:50), where *cis* was virtually grounded. Proteins, Ca²⁺/EGTA, and/or Na₂ATP were added to the *cis*. Transmembrane redox potentials were instilled by adding defined [GSH]/[GSSH] at on *cis* and *trans*, respectively. Both *cis* and *trans* were buffered to pH 7.4 with 10mM Hepes. Single-channel activity was measured using a patch-clamp amplifier (Bilayer Clamp BC 525C; Warner Instruments, Hampden, CT) at a holding potential of -40 mV applied to the

MOL #67959

trans chamber. The amplified current signals, filtered at 1 kHz (Low-Pass Bessel Filter 8 Pole; Warner Instruments) were digitized and acquired at a sampling rate of 10 kHz (Digidata 1320A; Molecular Devices, Sunnyvale, CA). All current recordings were made with Axoscope 10 software (Molecular Devices, Sunnyvale, CA) for at least 1 min under each experimental condition. The channel open probability (P_o), mean open times and mean closed-dwell times (t_o and t_c) were calculated using Clampfit, pClamp software 9.0 (Molecular Devices). The number of channels recorded under each *cis/trans* condition is specified in the respective figure legends. Differences in R163C and WT P_o were tested for statistical significance using unpaired Student's t-tests.

Results

Altered Ca^{2+} transient properties of skeletal myotubes, but not FDB fibers, isolated from R163C heterozygous mice

Primary myotubes cultured from WT and R163C heterozygous mice were challenged with electrical pulses ranging from 2-60 Hz at 25°C. Although both genotypes responded in a robust manner to electrical pulses, the amplitude of the Ca^{2+} transients were consistently lower in R163C myotubes compared to WT across the entire frequency range tested ($p < 0.01$; Fig 1A&B). Previously we reported that R163C myotubes exhibit a significantly higher rate of Mn^{2+} entry than WT during stimulation with a 20-Hz pulse train, and has been ascribed to enhanced ECCE in the mutant (Cherednichenko et al., 2008). Here we tested the magnitude of ECCE across a broad range of stimulus frequencies. R163C myotubes show significantly higher rates of ECCE between 2 Hz and 20 Hz compared to WT ($p < 0.005$; Fig 1C). However with stimuli >20 Hz R163C myotubes show a tendency

MOL #67959

for ECCE to plateau or decrease, whereas in WT myotubes ECCE increases throughout the stimulus range tested (i.e., the rate of Mn^{2+} entry increases with stimulus frequency between 2 and 60 Hz). In this regard, WT myotubes attain significantly higher rates of ECCE than R163C myotubes at 60 Hz ($p < 0.005$; Fig 1C).

In contrast to results obtained with myotubes, differences in the magnitude of electrically evoked Ca^{2+} transients did not differ between WT and R163C adult FDB fibers in the range of 1- 20 Hz when measured under the same experimental conditions (Fig 2A&B). As expected, FDB fibers isolated from R163C heterozygous mice exhibited a significantly amplified response to halothane challenge compared to WT under these experimental conditions, unmasking their MHS properties (Fig 2C & D).

Elevated $[Ca^{2+}]_{rest}$ in R163C myotubes and in vivo adult fibers

Microelectrode measurements showed that heterozygous R163C myotubes in culture have ~2.2-fold chronically elevated $[Ca^{2+}]_{rest}$ compared to their WT counterparts (Fig 3). Likewise, *in vivo* measurements of $[Ca^{2+}]_{rest}$ in the vastus lateralis of ketamine/xylazine anesthetized mice showed ~2.7-fold higher in R163C compared to $[Ca^{2+}]_{rest}$ in WT fibers (Fig 3).

RyR1, P-²⁸⁴⁴Ser-RyR1, FKBP12 and SERCA expression

Skeletal muscle membranes prepared from R163C knock-in and WT mice under basal (non-triggered) conditions were evaluated for the level of expression of RyR1 protein and its level of phosphorylation at ²⁸⁴⁴Ser (P-²⁸⁴⁴Ser). Figure 4A shows results from a typical western blot probed with monoclonal antibody 34C that recognizes RyR1, indicating no significant differences were detected in the level of RyR1 protein expression between the two genotypes (Fig 4A, green channel; Fig 4B summary data from n=29 blots from 5

MOL #67959

paired preparations). However, the same blots probed with an antibody that recognizes phosphorylation at ²⁸⁴⁴Ser (P-²⁸⁴⁴Ser-RyR1) showed a consistently significant higher signal with preparations obtained from heterozygous R163C compared to WT mice (Fig 4A, red channel). Quantitative analyses of the green and red channels by LI-COR imager identified 30.8% higher ratios of P-²⁸⁴⁴Ser-RyR1/total RyR1 in R163C preparations compared to those from WT (Fig 4C; $p < 0.001$).

In separate western blot experiments, the antibody that recognizes RyR1 was used in combination with an antibody that recognizes FKBP12 or SERCA1, respectively. The results showed that the ratio of total RyR1/FKBP12 immunoreactive protein was not significantly different between genotypes either in the level of FKBP12 (Fig 4D & E) or SERCA1 (Fig 4F&G) protein expression. Moreover, neither TG-sensitive Ca²⁺ ATPase activity (Fig 4H) nor the ratio of total RyR1/SERCA1 immunoreactive protein (data not shown) exhibited detectable differences between the two genotypes. Collectively these data suggested that although total RyR1, FKBP12 and SERCA1 protein expression were not significantly altered in R163C-RyR1 skeletal muscle, significantly elevated P-²⁸⁴⁴Ser-RyR1 were detected in R163C compared to WT.

RyR1-R163C channels have inherently higher open probability than WT

R163C- or WT- RyR1 channels were incorporated into BLM by induced fusion of SR vesicles. In the presence of 1mM free cytosolic (*cis*) Ca²⁺, 2mM Na₂ATP, and 100 μM free luminal (*trans*) Ca²⁺, the single channel activity was recorded at a holding potential of -40mV (applied to *trans*). Figure 5A (upper panel) shows representative current traces from a WT channel. Under these *cis/trans* conditions, the typical mean open probability (Po) of WT channels was Po=0.149±0.034 (n=9). In contrast, a total of n=23 independent

MOL #67959

reconstitutions of channels prepared from heterozygous R163C mouse skeletal muscle exhibited a significantly wider divergence of P_o values compared to WT. Successful reconstitutions from R163C membranes produced a frequency of channels that gated with significantly higher P_o than those reconstituted from WT (Fig 5A, lower traces). Of the 23 R163C channels recorded 13.0% exhibited P_o values that were ~2-fold higher than the mean P_o measured with WT channels, 30.4% exhibited P_o 2-4-fold higher than WT, and 21.7% exhibited >4-fold higher P_o than WT (Fig 5B). On the other hand, 34.8% of the R163C channels exhibited P_o values that were not statistically different ($p > 0.05$) from the mean behavior of channels reconstituted from WT (Fig 5B).

Dephosphorylation of RyR1-R163C has no significant effect on channel activity

The inherently higher P_o of R163C-RyR1 channels may be a consequence of the increased phosphorylation compared to WT channels. This hypothesis was directly tested by pretreatment of R163C and WT SR membranes with protein phosphatase 1 (PP1) (see Methods). Western blotting of total RyR1 and P-²⁸⁴⁴Ser-RyR1 showed near-complete dephosphorylation was achieved by PP1 pre-treatment in both genotypes, whereas sham incubations lacking PP1 preserved P-²⁸⁴⁴Ser-RyR1 and the higher level of phosphorylation in R163C preparations (Fig 6A). The functional consequence of dephosphorylation was analyzed using [³H]Ry binding analysis. Figure 6B shows that there are negligible differences between PP1-pretreated and sham treated membrane preparations from either genotype suggesting that phosphorylation and dephosphorylation had no significant effect on RyR1 channel activity.

[³H]Ry binding and regulation by Ca²⁺ is altered by the R163C mutation

Ca²⁺ is a physiological modulator of RyR1 channel activity. Ca²⁺ enhances [³H]Ry

MOL #67959

binding by interactions with high affinity (H) activation sites and inhibits the channel by interaction with allosterically coupled low affinity (L) sites, and facilitates removal of the inherent Mg^{2+} block (Voss et al., 2008). We examine if preparations from R163C differ from those from WT in their ability to bind [3H]Ry at high affinity sites and how an extended concentration range of Ca^{2+} (50nM to 10mM) influences this binding. Figure 5A shows that skeletal muscle membranes isolated from mice of both genotypes bound [3H]Ry in a Ca^{2+} dependent manner. Despite the fact that western blotting consistently indicated that skeletal muscle membrane preparations from WT and R163C mice showed no differences in total RyR1 protein expression (Fig 4A-C), R163C preparations attained higher [3H]Ry-binding levels at Ca^{2+} concentrations ranging from 0.2 to 1000 μ M. In the range of Ca^{2+} concentration optimal for [3H]Ry binding, R163C preparations showed ~2-fold higher maximum occupancy than WT (Fig 7A; $n=8$, $p < 0.0001$). Further analysis revealed that the EC_{50} for Ca^{2+} activation of [3H]Ry binding to R163C was 3-fold lower than that of WT ($EC_{50} = 0.5 \pm 0.1$ vs. 1.6 ± 0.4 μ M; $p < 0.01$; Fig 6B). On the other hand, the constant for Ca^{2+} inhibition of [3H]Ry binding (IC_{50}) did not differ between genotypes (331 ± 40 vs. 346 ± 31 μ M for R163C and WT, respectively (Fig 7B).

Sensitivity to Mg^{2+} inhibition remains unaltered in R163C

Cytoplasmic Mg^{2+} serves as a physiological negative modulator of RyR1 channel restricting channel Po both under resting and activating conditions (Lamb et al., 2001). Mg^{2+} inhibits RyR1 channel gating at physiological concentrations by competing with Ca^{2+} at both H and L sites (Laver et al., 1997a). Previously several studies showed that some MHS mutations reduce the potency of Mg^{2+} as a RyR1 channel inhibitor (Laver et al., 1997b). As expected, Mg^{2+} inhibited [3H]Ry binding to both R163C and WT in a dose-

MOL #67959

dependent manner (Fig 7C). Although baseline [^3H]Ry binding activity was significantly higher for R163C than that of WT in the absence of Mg^{2+} , binding was completely inhibited by $\text{Mg}^{2+} \geq 5\text{mM}$ for both genotypes. Further analysis revealed that IC_{50} values did not differ between R163C and WT ($410 \pm 23 \mu\text{M}$ vs. $395 \pm 28 \mu\text{M}$, respectively; Fig 7D).

R163C responds to redox regulation

In healthy cells, highly reduced cytosolic glutathione redox potentials ($\sim 220\text{-}230\text{mV}$) help maintain low RyR1 channel gating activity under resting conditions (Hwang et al., 1995). RyR1 channels are regulated by glutathione redox status possibly mediated by glutathionylation and/or nitration of hyper-reactive sulfhydryl residues within the channel complex (Marengo et al., 1998; Feng et al 2000). We assessed how reducing or oxidizing [GSH]/[GSSG] conditions influenced the apparent association rate of [^3H]Ry to R163C and WT preparations. Figure 8A shows the initial association of [^3H]Ry over the first 15 min of incubation at 37°C in the presence of optimal Ca^{2+} ($50 \mu\text{M}$) in the assay medium. The bimolecular association (pseudo-first order) rate constants (k_{obs}) were calculated (Fig 8B). Preparations from R163C mice had significantly faster k_{obs} than those prepared from WT mice when measured in the presence of oxidizing glutathione, GSSG (5mM) ($k_{\text{obs}} = 19.0 \pm 1.9$ vs. 11.8 ± 1.1 fmole/mg/min, respectively; $p < 0.01$). Although the relative magnitude of the reduction of [^3H]Ry-binding rates in an assay medium containing reducing GSH (5mM) compared to one containing GSSG were similar in both genotypes (Fig 8A and 8B; $\sim 62.2\text{-}67.8\%$ $n=6\text{-}8$), the k_{obs} measured in R163C-RyR1 preparations in reducing buffer was nearly identical to the k_{obs} measured with WT-RyR1 in an oxidizing buffer (Fig 8A and 8B). This suggests that the R163C channels are inherently hyperactive, even in the presence of a highly reducing [GSH]/[GSSG] buffer.

MOL #67959

To further test if R163C maintains responses to redox regulation, we focused our comparison on reconstituted R163C channels that possessed P_o >3-fold of WT under standard buffer conditions (*cis* 1 μ M Ca^{2+} , 2mM ATP/ *trans* 100 μ M Ca^{2+}) with undefined *cis/trans* redox potential (no GSH or GSSG added to the solutions). Analysis of n=6 R163C independent single channel experiments showed that channels with this mutation maintained a significantly higher mean P_o compared to WT in the presence of a highly reducing [GSH]/[GSSG] potential on the cytoplasmic side (* $p=0.024$, left Y-axis Fig 8C). However, both R163C and WT channels responded with a similar reduction in P_o once transmembrane redox potential was adjusted to a reducing [GSH]/[GSSG] potential on the cytoplasmic side relative to their respective baseline period (in an undefined redox potential) ($p=0.149$, right Y-axis Fig 8C). Collectively these results indicate that R163C channels remain responsive to changes in *cis* redox potential but maintain significantly higher P_o than WT channels even under highly reducing redox potential, indicating that channels with the R163C mutation are inherently hyperactive.

Influence of temperature on [³H]Ry binding kinetics

Since temperature may be a critical factor in triggering MH in susceptible individuals, we compared the apparent rate (k_{obs}) of [³H]Ry binding at two temperatures, 25°C and 37°C. Figure 10 shows that as expected k_{obs} was significantly slower at 25°C than at 37°C for both heterozygous R193C and WT genotypes. Interestingly the k_{obs} for R163C was 1.5-fold faster at 37°C, and 2-fold faster at 25°C when compared to the k_{obs} values obtained from WT at the respective temperatures.

MOL #67959

Discussion

The R163C mutation is one of the five most common mutations conferring MHS in humans (Robinson et al., 2006). This study identifies several impairments inherent to the regulation of R163C RyR1 isolated from skeletal muscle of heterozygous mice in the absence of triggering agents. Most notable is the significantly higher single channel activity exhibited by R163C compared to WT. If one assumes that RyR1 monomers composed of WT and R163C gene products randomly associate to form functional channel tetramers, then five distinct combinations of WT and R163C monomers could contribute to divergent channel gating behaviors in BLM experiments with SR prepared from heterozygous R163C. In fact, ~35% of the R163C channels reconstituted in BLM were found to possess open probabilities not significantly different from those measured for channels prepared from WT skeletal muscle under the defined experimental conditions used in this study. The remaining 65% of the channels measured had 2- to >4-fold higher P_o values ($p < 0.05$) than WT. This distribution of P_o values suggests that a ratio of 1 R163C:3 WT monomers within a channel tetramer may alter channel P_o in a subtle manner difficult to resolve given the limitations of the BLM method. Nevertheless, the divergence of P_o values observed in 65% of the channels recorded may reflect a gene-dose effect, with tetramers composed of 2:2, 3:1 and 4:0 ratios of R163C:WT monomers increasing the probability of transitions to the channel open state.

Due to birth lethality in R163C homozygous mice, this hypothesis could not be directly tested in SR prepared from adult skeletal muscle. Binding studies with [^3H]Ry indicate that membranes prepared from R163C mice bind significantly more (2-fold) radioligand in the presence of an optimal Ca^{2+} buffer compared to WT. This difference in

MOL #67959

occupancy is not a result of differential expression of protein in R163C preparations, as the levels of RyR1 immunoreactive protein did not differ between the genotypes when measured in the same preparations used for binding analysis. Collectively these data indicate that the majority of R163C channels recovered from heterozygous mice have inherently higher activity than WT.

A possible contributor leading to enhanced channel activity was the significantly higher levels of phosphorylation at ²⁸⁴⁴Ser observed with R163C-RyR1. Phosphorylation of RyR1 destabilized interactions with FKBP12 and was associated enhanced channel activity (Reiken et al., 2003) and promotes RyR1 channel substate behavior (Marx et al., 2000). Thus one possible mechanism that may contribute to destabilization of the closed state of R163C channels is the loss of FKBP12, even in the absence of triggering agents.

However, our results with R163C-RyR1 don't support this hypothesis since the ratio of FKBP12/RyR1 did not differ in heavy SR preparations from R163C and WT. Moreover, R163C channels remained responsive to bastadin 5 (n=4 of 4 R163C-RyR1 channels; unpublished observation), a compound known to activate RyR1 channel in FKBP12-dependent manner (Mack et al., 1994). Dephosphorylation of RyR1 with exogenous PP1 had little effect on [³H]Ry binding to either genotype, despite the near-complete loss of signal using the phospho-²⁴⁸⁸Ser-RyR1 antibody. Further, PP1 added to RyR1 preparations before or after single channels were reconstituted in BLM failed to reduce the channel Po of either WT or R163C preparations in continuous recordings lasting 20-60min (in preparation). Thus increased phosphorylation of R163C-RyR1 compared to WT under basal conditions (i.e., in the absence of triggering agent) has little influence on the amount of FKBP12 associated, and therefore cannot directly account for the pronounced

MOL #67959

differences in channel behavior observed between these genotypes. Although ours is the first evidence that the phosphorylation level at ²⁸⁴⁴Ser-RyR1 is not associated with impaired binding of FKBP12, a similar conclusion was reached based on the lack of measureable effect of PKA-dependent RyR2 phosphorylation on binding of either FKBP12 or 12.6 in cardiomyocytes (Guo et al., 2010).

Heightened sensitivity to activation by cytoplasmic Ca²⁺ is the prominent characteristic of R163C channels, even under highly reducing redox potentials, and may reflect a lowered energy barrier needed for opening the channel and unmasking high-affinity binding sites for ryanodine. Although high-affinity binding of [³H]Ry and channel activity are low when cytoplasmic Ca²⁺ is adjusted ≤100 nM, R163C myotubes and adult fast twitch fibers maintain a chronically elevated [Ca²⁺]_{rest}. Therefore at resting condition, when [Ca²⁺]_{rest} is >200 nM, the influence of R163C on high-conductance channel gating would be most pronounced during Ca²⁺ release triggered by EC coupling as Ca²⁺ on the cytoplasmic face of the channel increases. Expression of RyR1 is responsible for more than half of total [Ca²⁺]_{rest} measured in WT myotubes (Eltit et al., 2010), and MHS mutations significantly raise [Ca²⁺]_{rest} compared to WT (Yang et al., 2007b) that may arise from the RyR1 ryanodine-insensitive Ca²⁺ leak conformation (Pessah et al., 1997). Thus altered regulation of R163C by Ca²⁺ is likely to contribute to the pronounced destabilizing effects of agents that trigger MH. Contrary to previous results obtained from [³H]Ry binding and single channel analyses of SR prepared from homozygous porcine R615C (Balog et al., 2001) and R163C expressed in 1B5 RyR-null myotubes (Yang et al., 2006), we did not find significant shifts in either inhibition by Mg²⁺ or high Ca²⁺ compared to WT. Whether the divergence reflects zygosity, the penetrance of the two mutations, and/or species

MOL #67959

differences remains unclear.

Considering the higher sensitivity of R163C channels to Ca^{2+} and the inability of physiological reducing potentials to restore the low P_o gating state seen in WT, it suggests that R163C channels possessing R163C mutation(s) are inherently hyperactive. Channel hyperactivity could be the consequence of complex mechanisms that involve glutathionylation and nitrosylation of RyR1 at reactive cysteines (Durham et al., 2008), but does not appear to be a direct consequence of increased phosphorylation. The allosteric structural changes caused by the R163C mutation could promote formation and stabilize inappropriate disulfide bond(s) with reactive Cys normally present in RyR1 (Feng et al., 2000; Voss et al., 2004) and/or disrupt intra or inter subunit interactions (Tung et al., 2010). In the present study we did not discriminate which of these mechanisms contributes to channel dysfunction. Nevertheless, since triggering fulminant MH is associated with oxidative bursts, ineffective regulation of R163C channels by glutathione may not only contribute to uncontrolled release of SR Ca^{2+} , but also further promote it.

To our knowledge the present study is the first to examine how functional dysregulation of a common heterozygous MHS mutation influences EC coupling behavior in intact myotubes and adult skeletal muscle fibers derived from the same animals. R163C has a clearly observable influence on EC coupling in myotubes, but not adult FDB fibers. Significantly depressed Ca^{2+} transient amplitudes observed at all stimulus frequencies (1-60 Hz) is consistent with the recent report of Bannister et al (Bannister et al., 2010b) using voltage clamp of R163C and WT myotubes. The reduced amplitudes elicited by electrical stimuli seen with R163C could result from partial depletion of SR Ca^{2+} stores conferred by MHS SR that is chronically more leaky to Ca^{2+} than WT in the affected myotubes

MOL #67959

(Bannister et al., 2010b). Previously we reported that excitation-coupled Ca^{2+} entry (ECCE) in R163C myotubes was significantly enhanced compared to WT (Cherednichenko et al., 2008). Here we extend these finding over a broad range of stimulus frequencies and report that although enhanced ECCE occurs at stimuli ≤ 20 Hz, at higher frequencies ECCE begins to fail and is associated with failure to maintain the Ca^{2+} transient amplitude during a 10 sec 60 Hz pulse train. One possible contributor to the failure of ECCE at high frequencies may be related to the delay in the inactivation process (Bannister et al., 2010a). The present study supports that altered bidirectional signaling between DHPR and RyR1 contribute to the MHS phenotype.

An unexpected observation is that Ca^{2+} transient amplitudes measured in heterozygous R163C FDB fibers do not differ from their WT counterpart in the stimulus range tested, consistent with contractility measurements made at 25°C with soleus fibers isolated from heterozygous Y522S and WT mice (Chelu et al., 2006). Our analyses of [^3H]Ry binding show a significantly greater K_{obs} (pseudo-first order rate) for R163C at either 25°C or 37°C, indicating inherent channel dysfunction occurs at lower than physiological temperatures.

Perhaps the lack of a detectible impairment in the Ca^{2+} transient phenotype of FDB fibers when assayed under basal conditions should not be considered unexpected given that heterozygous R163C mice do not exhibit an overt phenotype throughout their lifespan in the absence of temperature stress or triggering agent. One possible explanation for the divergence in EC coupling deficit seen in myotubes and adult FDB fibers from heterozygous R163C mice is that adult fibers have more developed Ca^{2+} release units than myotubes (Flucher and Franzini-Armstrong, 1996). Moreover myotubes express

MOL #67959

RyR1 splice variants not found in adult fibers that magnify depolarization-dependent Ca^{2+} release (Kimura et al., 2009). On the other hand, myotubes express a high conductance $\alpha 1$ Cav1.1 isoform not found in adult fibers (Tuluc et al., 2009). The rather remarkable dysfunction of R163C channels measured from SR preparations prepared from adult mice must be limited by strong negative regulation in context of the Ca^{2+} release unit of adult fibers, and to a lesser extent, in myotubes where the junctions are less developed and have different CRU composition. This hypothesis is consistent with previous data that identifies the DHPR as a strong negative regulatory module of RyR1 (Zhou et al., 2006). This possibility could explain the pharmacogenic nature of MH; a lack of overt phenotype under basal physiologic circumstances despite the presence of inherently dysregulated RyR1 channels. The rapid appearance of fulminant life-threatening MH in response to temperature stress and triggering agents could be mediated by weakening of the negative feedback provided by DHPR thereby unmasking the full dysfunction of MHS RyR1. This hypothesis deserves investigation.

Author Contributions:

Wei Feng: Participated in research design, conducted experiments, performed data analysis, contributed to writing the manuscript

Genaro C. Barrientos: Participated in research design, conducted experiments, performed data analysis, contributed to writing the manuscript

Gennady Cherednichenko: Participated in research design, conducted experiments, performed data analysis, contributed to writing the manuscript

Tianzhong Yang: Contributed novel reagents

Isela T. Padilla: Conducted experiments, performed data analysis

Kim Truong: Conducted experiments, performed data analysis

Paul D. Allen: Contributed novel reagents, contributed to writing the manuscript

José R. Lopez: Conducted experiments, performed data analysis

Isaac N. Pessah: Participated in research design, performed data analysis, contributed to writing the manuscript

MOL #67959

References

- Airey JA, Beck CF, Murakami K, Tanksley SJ, Deerinck TJ, Ellisman MH and Sutko JL (1990) Identification and localization of two triad junctional foot protein isoforms in mature avian fast twitch skeletal muscle. *J Biol Chem* **265**:14187-14194.
- Balog EM, Fruen BR, Shomer NH and Louis CF (2001) Divergent effects of the malignant hyperthermia-susceptible Arg(615)-->Cys mutation on the Ca(2+) and Mg(2+) dependence of the RyR1. *Biophys J* **81**:2050-2058.
- Bannister RA, Esteve E, Eltit JM, Pessah IN, Allen PD, Lopez JR and Beam KG (2010a) A malignant hyperthermia-inducing mutation in RYR1 (R163C): consequent alterations in the functional properties of DHPR channels. *J Gen Physiol* **135**:629-640.
- Brown LD, Rodney GG, Hernandez-Ochoa E, Ward CW and Schneider MF (2007) Ca²⁺ sparks and T tubule reorganization in dedifferentiating adult mouse skeletal muscle fibers. *Am J Physiol Cell Physiol* **292**:C1156-1166.
- Buck ED, Nguyen HT, Pessah IN, Allen PD (1997) Dyspedic mouse skeletal muscle expresses major elements of the triadic junction but lacks detectable ryanodine receptor protein and function. *J Biol Chem* **272**:7360-7367.
- Chelu MG, Goonasekera SA, Durham WJ, Tang W, Lueck JD, Riehl J, Pessah IN, Zhang P, Bhattacharjee MB, Dirksen RT and Hamilton SL (2006) Heat- and anesthesia-induced malignant hyperthermia in an RyR1 knock-in mouse. *FASEB J* **20**:329-330.
- Cherednichenko G, Hurne AM, Fessenden JD, Lee EH, Allen PD, Beam KG and Pessah IN (2004) Conformational activation of Ca²⁺ entry by depolarization of skeletal myotubes. *Proc Natl Acad Sci U S A* **101**:15793-15798.
- Cherednichenko G, Ward CW, Feng W, Cabrales E, Michaelson L, Samsó M, Lopez JR, Allen PD and Pessah IN (2008) Enhanced excitation-coupled calcium entry in myotubes expressing malignant hyperthermia mutation R163C is attenuated by dantrolene. *Mol Pharmacol* **73**:1203-1212.
- Dulhunty AF, Laver D, Curtis SM, Pace S, Haarmann C and Gallant EM (2001) Characteristics of irreversible ATP activation suggest that native skeletal ryanodine receptors can be phosphorylated via an endogenous CaMKII. *Biophys J* **81**:3240-3252.
- Durham WJ, Aracena-Parks P, Long C, Rossi AE, Goonasekera SA, Boncompagni S, Galvan DL, Gilman CP, Baker MR, Shirokova N, Protasi F, Dirksen R and Hamilton SL (2008) RyR1 S-nitrosylation underlies environmental heat stroke and sudden death in Y522S RyR1 knockin mice. *Cell* **133**:53-65.
- Eltit JM, Yang T, Li H, Molinski TF, Pessah IN, Allen PD and Lopez JR (2010) RyR1-mediated Ca²⁺ leak and Ca²⁺ entry determine resting intracellular Ca²⁺ in skeletal myotubes. *J Biol Chem* **285**:13781-13787.
- Esteve E, Eltit JM, Bannister RA, Liu K, Pessah IN, Beam KG, Allen PD and Lopez JR (2010a) A malignant hyperthermia-inducing mutation in RYR1 (R163C): alterations in Ca²⁺ entry, release, and retrograde signaling to the DHPR. *J Gen Physiol* **135**:619-628.
- Feng W, Liu G, Allen PD and Pessah IN (2000) Transmembrane redox sensor of ryanodine receptor complex. *J Biol Chem* **275**:35902-35907.

MOL #67959

- Flucher BE and Franzini-Armstrong C (1996) Formation of junctions involved in excitation-contraction coupling in skeletal and cardiac muscle. *Proc Natl Acad Sci U S A* **93**:8101-8106.
- Guo T, Cornea RL, Huke S, Camors E, Yang Y, Picht E, Fruen BR, Bers DM (2010) Kinetics of FKBP12.6 binding to ryanodine receptors in permeabilized cardiac myocytes and effects on Ca sparks. *Circ Res.* 106:1743-52.
- Hwang C, Lodish HF and Sinskey AJ (1995) Measurement of glutathione redox state in cytosol and secretory pathway of cultured cells. *Methods Enzymol* **251**:212-221.
- Kimura T, Lueck JD, Harvey PJ, Pace SM, Ikemoto N, Casarotto MG, Dirksen RT and Dulhunty AF (2009) Alternative splicing of RyR1 alters the efficacy of skeletal EC coupling. *Cell Calcium* **45**:264-274.
- Lamb GD, Posterino GS, Yamamoto T and Ikemoto N (2001) Effects of a domain peptide of the ryanodine receptor on Ca²⁺ release in skinned skeletal muscle fibers. *Am J Physiol Cell Physiol* **281**:C207-214.
- Laver DR, Baynes TM and Dulhunty AF (1997a) Magnesium inhibition of ryanodine-receptor calcium channels: evidence for two independent mechanisms. *J Membr Biol* **156**:213-229.
- Laver DR, Owen VJ, Junankar PR, Taske NL, Dulhunty AF and Lamb GD (1997b) Reduced inhibitory effect of Mg²⁺ on ryanodine receptor-Ca²⁺ release channels in malignant hyperthermia. *Biophys J* **73**:1913-1924.
- Lehmann-Horn F, Jurkat-Rott K and Rudel R (2008) Diagnostics and therapy of muscle channelopathies--Guidelines of the Ulm Muscle Centre. *Acta Myol* **27**:98-113.
- Mack MM, Molinski TF, Buck ED, and Pessah IN (1994) Novel modulators of skeletal muscle FKBP12/calcium channel complex from lanthella basta: Role of FKBP12 in channel gating. *J Biol Chem* **269**:23236-23249.
- Marengo JJ, Hidalgo C and Bull R (1998) Sulfhydryl oxidation modifies the calcium dependence of ryanodine-sensitive calcium channels of excitable cells. *Biophys J* **74**:1263-1277.
- Marx SO, Reiken S, Hisamatsu Y, Jayaraman T, Burkhoff D, Rosemblyt N and Marks AR (2000) PKA phosphorylation dissociates FKBP12.6 from the calcium release channel (ryanodine receptor): defective regulation in failing hearts. *Cell* **101**:365-376.
- Pessah IN, Molinski TF, Meloy TD, Wong P, Buck ED, Allen PD, Mohr FC, and Mack MM (1997) Bastadins relate ryanodine-sensitive and ryanodine-insensitive "leak" Ca²⁺ efflux pathways in skeletal SR and BC₃H1 cells. *Amer. J. Physiol. (Cell Physiol.)* **272**:C601-C614.
- Protasi F (2002) Structural interaction between RYRs and DHPRs in calcium release units of cardiac and skeletal muscle cells. *Front Biosci* **7**:d650-658.
- Reiken S, Lacampagne A, Zhou H, Kherani A, Lehnart SE, Ward C, Huang F, Gaburjakova M, Gaburjakova J, Rosemblyt N, Warren MS, He KL, Yi GH, Wang J, Burkhoff D, Vassort G and Marks AR (2003) PKA phosphorylation activates the calcium release channel (ryanodine receptor) in skeletal muscle: defective regulation in heart failure. *J Cell Biol* **160**:919-928.
- Robinson R, Carpenter D, Shaw MA, Halsall J and Hopkins P (2006) Mutations in RYR1 in malignant hyperthermia and central core disease. *Hum Mutat* **27**:977-989.
- Robinson RL, Anetseder MJ, Brancadoro V, van Broekhoven C, Carsana A, Censier K, Fortunato G, Girard T, Heytens L, Hopkins PM, Jurkat-Rott K, Klinger W, Kozak-

MOL #67959

- Ribbens G, Krivosic R, Monnier N, Nivoche Y, Olthoff D, Rueffert H, Sorrentino V, Tegazzin V and Mueller CR (2003) Recent advances in the diagnosis of malignant hyperthermia susceptibility: how confident can we be of genetic testing? *Eur J Hum Genet* **11**:342-348.
- Sheridan DC, Takekura H, Franzini-Armstrong C, Beam KG, Allen PD and Perez CF (2006) Bidirectional signaling between calcium channels of skeletal muscle requires multiple direct and indirect interactions. *Proc Natl Acad Sci U S A* **103**:19760-19765.
- Ta TA, Feng W, Molinski TF and Pessah IN (2006) Hydroxylated xestospongins block inositol-1,4,5-trisphosphate-induced Ca²⁺ release and sensitize Ca²⁺-induced Ca²⁺ release mediated by ryanodine receptors. *Mol Pharmacol* **69**:532-538.
- Takeshima H, Iino M, Takekura H, Nishi M, Kuno J, Minowa O, Takano H and Noda T (1994) Excitation-contraction uncoupling and muscular degeneration in mice lacking functional skeletal muscle ryanodine-receptor gene. *Nature* **369**:556-559.
- Tuluc P, Molenda N, Schlick B, Obermair GJ, Flucher BE and Jurkat-Rott K (2009) A CaV1.1 Ca²⁺ channel splice variant with high conductance and voltage-sensitivity alters EC coupling in developing skeletal muscle. *Biophys J* **96**:35-44.
- Tung C-C, Lobo PA, Kimlicka L, and Petegem FV (2010) The amino-terminal disease hotspot of ryanodine receptors forms a cytoplasmic vestibule. *Nature* Nov 3. [Epub ahead of print] PMID: 21048710
- Voss AA, Allen PD, Pessah IN and Perez CF (2008) Allosterically coupled calcium and magnesium binding sites are unmasked by ryanodine receptor chimeras. *Biochem Biophys Res Commun* **366**:988-993.
- Voss AA, Lango J, Ernst-Russell M, Morin D, and Pessah IN (2004) Identification of Hyperreactive Cysteines within Ryanodine Receptor Type 1 by Mass Spectrometry. *J Biol Chem* **279**:34514-20.
- Yang T, Allen PD, Pessah IN and Lopez JR (2007a) Enhanced excitation-coupled calcium entry in myotubes is associated with expression of RyR1 malignant hyperthermia mutations. *J Biol Chem* **282**:37471-37478.
- Yang T, Esteve E, Pessah IN, Molinski TF, Allen PD and Lopez JR (2007b) Elevated resting [Ca²⁺]_i in myotubes expressing malignant hyperthermia RyR1 cDNAs is partially restored by modulation of passive calcium leak from the SR. *Am J Physiol Cell Physiol* **292**:C1591-1598.
- Yang T, Riehl J, Esteve E, Matthei KI, Goth S, Allen PD, Pessah IN and Lopez JR (2006) Pharmacologic and functional characterization of malignant hyperthermia in the R163C RyR1 knock-in mouse. *Anesthesiology* **105**:1164-1175.
- Zhou J, Allen, P. D., Pessah, I. N., Naguib, M. (2010) Neuromuscular disorders and malignant hyperthermia, in *Miller's Anesthesia* (Miller RD ed) p 1171, Churchill Livingstone, Philadelphia
- Zhou J, Brum G, Gonzalez A, Launikonis BS, Stern MD and Rios E (2005) Concerted vs. sequential. Two activation patterns of vast arrays of intracellular Ca²⁺ channels in muscle. *J Gen Physiol* **126**:301-309.
- Zhou J, Yi J, Royer L, Launikonis BS, Gonzalez A, Garcia J and Rios E (2006) A probable role of dihydropyridine receptors in repression of Ca²⁺ sparks demonstrated in cultured mammalian muscle. *Am J Physiol Cell Physiol* **290**:C539-553.

MOL #67959

Footnotes

* Contributed equally to the manuscript

Supported by National Institute of Arthritis and Musculoskeletal and Skin Disease [AR46513 and AR52354] and the National Institute of Environmental Health Sciences [ES014901 and ES04699].

MOL #67959

Figure Legends

Figure 1. Myotubes isolated for R163C heterozygous and WT mice differ in their responses to electrical stimuli. **A.** Skeletal myotubes were stimulated by electrical field at 1 to 60 Hz and Ca^{2+} transients measured with Fluo-4 monitored at 25°C as described in Methods. Shown are representative responses to 1, 5, 20 and 60 Hz from WT (black trace) and R163C myotubes (grey trace). **B.** Summary data showing mean \pm SEM of normalized Ca^{2+} transient amplitudes for WT (n= 21 cells) and R163C (n=24 cells) measured from at least 3 different cultures. The transient amplitude elicited in R163C myotubes was significantly lower than WT at all stimulation frequencies ($p < 0.01$). **C.** Electrically evoked Mn^{2+} entry was measured during field stimulation at 2 to 60 Hz using the quench of Fura-2 fluorescence as described in Methods. The rate of Mn^{2+} entry was significantly greater in R163C compared to WT myotubes with 2, 10, 20, 40 and 60 Hz stimuli ($p < 0.01$), whereas the rate of Mn^{2+} quench was significantly lower in R163C compared to WT with a 60 Hz stimulus ($p < 0.005$). Data shown are means (\pm SEM) from n=8 to 29 myotubes measured at each frequency.

Figure 2. Adult FDB fibers isolated for R163C heterozygous MHS and WT mice do not differ in their responses to electrical stimuli. **A.** Representative traces showing the frequency responses in WT (black traces) and R163C (grey traces) FDB fibers. Fibers were loaded with Fluo-4 and Ca^{2+} responses were elicited by electric field stimulation at 1, 2.5, 5, 10 and 20 Hz (10 s duration) as described in Methods. **B.** For each stimuli frequency the integrated area was calculated and plotted as mean \pm SEM. WT n=68 from 4 different fiber isolations, R163C n=78 from 2 different fiber isolations. **C.** Representative

MOL #67959

trace showing that FDB fibers isolated from R163C show an amplified response to acute challenge with 0.1% halothane in the perfusion medium compared to FDB isolated from WT mice. **D.** Amplitude of the Ca^{2+} response 30 sec following the start of perfusion with halothane (0.1%). The magnitude of halothane-induced Ca^{2+} release was normalized to the baseline of each fiber 10 sec before commencing perfusion of halothane. The data shown are mean (\pm SEM) obtained from $n=16$ R163C and $n=24$ WT fibers from 2 separate isolations ($***p < 0.001$).

Figure 3. Elevated $[\text{Ca}^{2+}]_{\text{rest}}$ in heterozygous R163C myotubes and adult fibers

Microelectrode measurements of $[\text{Ca}^{2+}]_{\text{rest}}$ in cultured myotubes and in adult vastus lateralis fibers *in vivo* were made as described in Methods. The data shown are mean \pm SEM $[\text{Ca}^{2+}]_{\text{rest}}$ values which differed significantly between WT and R163C for both cultured myotubes and adult fibers ($***p < 0.001$).

Figure 4. No differences in total RyR1, FKBP12 and SERCA expression, but enhanced phosphorylation of $^{2844}\text{Ser-RyR1}$ in preparations from R163C heterozygous compared to those from WT mice.

A. Representative western blot from five independent preparations showing the expression of RyR1 probed with monoclonal 34C (total RyR1; green channel) and an antibody that selectively recognizes phosphorylated $^{2844}\text{Ser-RyR1}$ ($\text{P-}^{2844}\text{Ser-RyR1}$; red channel). **B.** Densitometry results show no differences between R163C and WT for total RyR1 protein expression. Bar graph represents the mean \pm SEM for $n=21$ blots from 7 membrane preparations. **C.** Densitometry results show that R163C has significantly higher levels of $\text{P-}^{2844}\text{Ser-RyR1}$ compared to WT. $\text{P-}^{2844}\text{Ser-RyR1}$ signal (red channel) was

MOL #67959

normalized to total RyR1 (green channel for each western blot. The bar graph represents the mean \pm SEM for n=29 blots from 5 membrane preparations. **D.** Representative western blot showing RyR1 (green channel) and FKBP12 (red channel). **E.** Mean \pm SD densitometry results from WT (n=8) and R163C (n=10) of two paired protein preparations. **F.** Representative western blot showing the SERCA1 expression from three separate preparations from WT and R163C mice. For each sample 5 μ g of protein was loaded per lane. **G.** Mean \pm SEM densitometry results from n=4 preparations per genotype replicated in triplicate. **H.** Mean \pm SEM of the Ca²⁺-ATPase activity measured in an assay that couples Ca²⁺-dependent ATP hydrolysis to NADH oxidation (coupled enzyme assay) described in Methods. The initial rate of NADH oxidation are shown for n=6 determinations for WT and R163C. Specificity was assessed thapsigargin (TG). >95% of the initial rate of NADH oxidation was TG-sensitive.

Figure 5. RyR1 channels reconstituted from R163C preparations have high open probabilities. Single channels were fused with BLM from SR vesicles prepared from either WT or R163C heterozygous mouse skeletal muscles. In **A**, the gating behavior of a representative WT channel (upper traces) is contrasted with a R163C channel (lower traces) that exhibited >4-fold higher Po and was representative of ~22% of the R163C channel reconstituted. The channels were recorded for \geq 1 min at -40 mV holding potential applied to *trans*, with *cis* solution (cytosolic) containing 1 μ M free (*cis*) Ca²⁺ and 2 mM ATP, and *trans* (luminal) containing 100 μ M free Ca²⁺. Open probability (Po) was obtained from analysis of individual channel by pClamp 9.0 software. Arrows with “o” or “c” indicate the maximal current amplitude when the channel is fully opened or closed, respectively. **B.** Summary of Po analysis from n=9 WT and n=23 R163C channels recorded under identical

MOL #67959

experimental conditions. R163C channels exhibiting ≥ 2 -fold P_o compared to WT were statistically significantly at $p < 0.05$ using unpaired Student's t-test.

Figure 6. Dephosphorylation of either R163C- or WT RyR1 with protein phosphatase 1 (PP1) has negligible influence on [³H]Ry binding activity. SR from R163C and WT were pre-incubated with and without PP1, and subsequent analyzed using [³H]Ry binding as described in Methods. **A.** Representative western blot results (n=2). **B.** [³H]Ry binding results mean \pm SD from n=6 of two paired protein preparations. Statistic analysis indicated no significant difference between the samples pretreated without or with PP1 with preparations from either genotype.

Figure 7. R163C exhibits altered [³H]Ry binding and Ca²⁺ activation, but inhibition by Ca²⁺ and Mg²⁺ remains unaltered. Equilibrium [³H]ryanodine (2nM) binding to 100mg/ml SR protein was performed at 37°C, 3 hours in the presence of 50nM-10mM Ca²⁺. Free Ca²⁺ was adjusted by EGTA according the software Bound and Determined (Voss et al., 2008). The data points were mean \pm SD from n=6 determinations from two independent membrane preparations from paired R163C heterozygous and WT mice. **A** and **B** show raw data and corresponding data normalized to the maximum binding within each genotype. **C** and **D.** Mg²⁺ (0-20mM) inhibits equilibrium [³H]Ry binding. The free Ca²⁺ in the reaction mixture was buffered by EGTA. The data points were mean \pm SD from n=6 determinations from two independent membrane preparations from paired R163C heterozygous and WT mice.

MOL #67959

Figure 8. Response of R163C channels to glutathione redox potential. Reducing and oxidizing conditions were set in the assay buffer by addition of 5mM GSH and 5mM GSSG, respectively. [³H]Ry (5nM) was added to the assay buffer to initiate the binding and the reaction quenched at the indicated time points by filtration. The binding reaction was terminated at 0, 3, 6, 9, 12, 15 min and the results were plotted in **A**. The pseudo-first order binding rates (k_{obs}) were obtained from the linear fitting and plotted as bar graphs in **B** (n=6-8 determinations). **C**. Summarizes analysis of single channel Po in the presence of a transmembrane redox potential set at -230mv/-180mV (*cis/trans*) for n=6 independent R163C and WT channels reconstituted in BLM (left Y-axis label). The respective changes in Po when the transmembrane redox potential was set at -230mv/-180mV (*cis/trans*) relative to the corresponding control period for WT (n=6) and R163C (n=6) channels are shown (right Y-axis label). Mean±SD are shown and were not statistically different between the two genotypes (p=0.149). Statistical analyses indicate where significant differences were found using independent Student's t-tests (** $p < 0.01$; *** $p < 0.001$).

Figure 9. Influence of temperature on [³H]ry binding kinetics to R163C and WT preparations. Binding of 5nM [³H]Ry to 100µg/ml of SR preparations was initiated at either 25°C or 37°C and quenched at 5, 10, 15, 20, 25 and 30 min. The rate lines were plotted in the left panel. The initial rates were obtained from linear curve fitting (left panel) and the calculated k_{obs} values plotted as bar graphs in the right panel. Statistical analyses indicate significant difference among the compared groups (*** $p < 0.001$; n=6-8).

Skeletal Myotubes

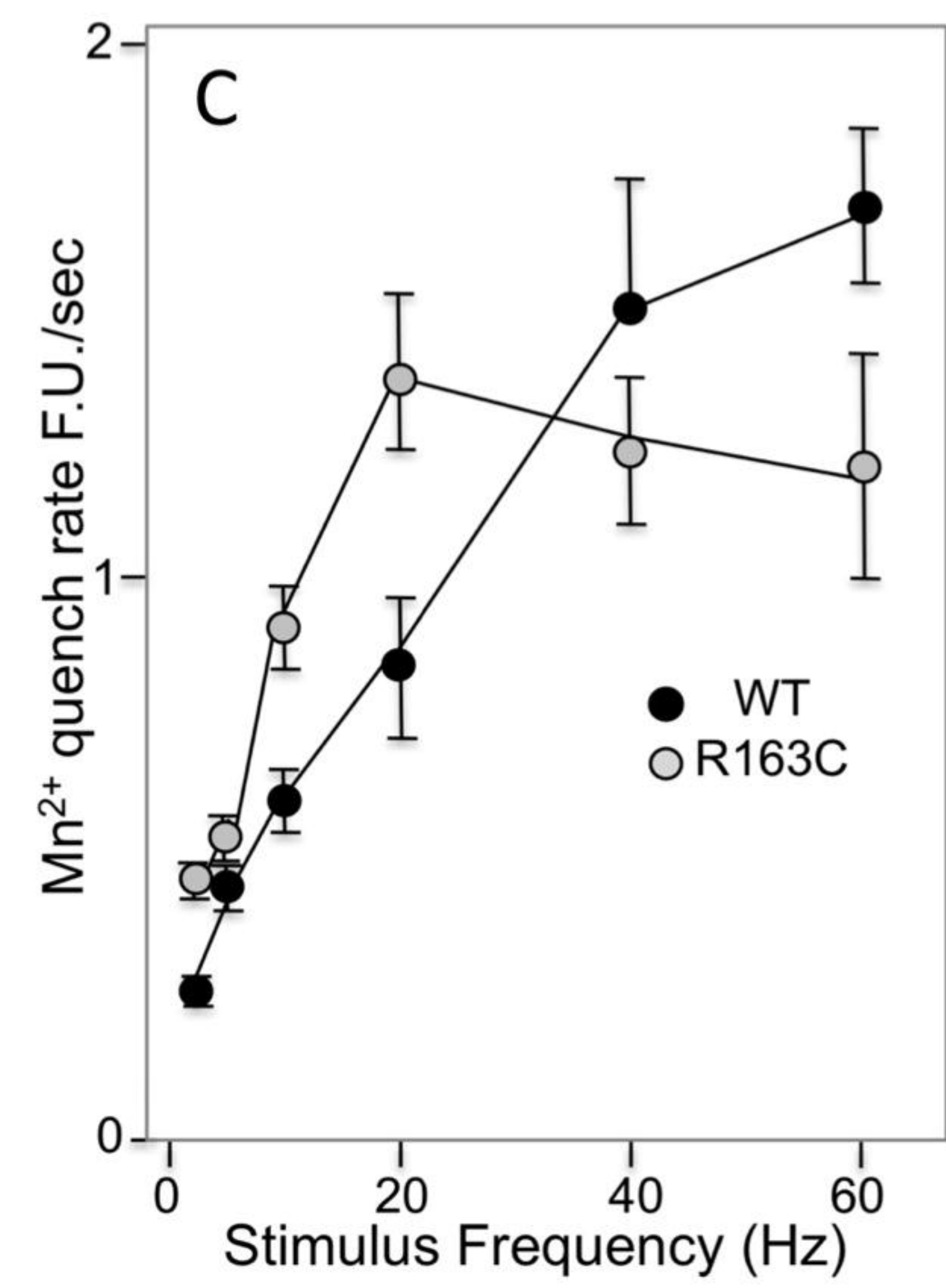
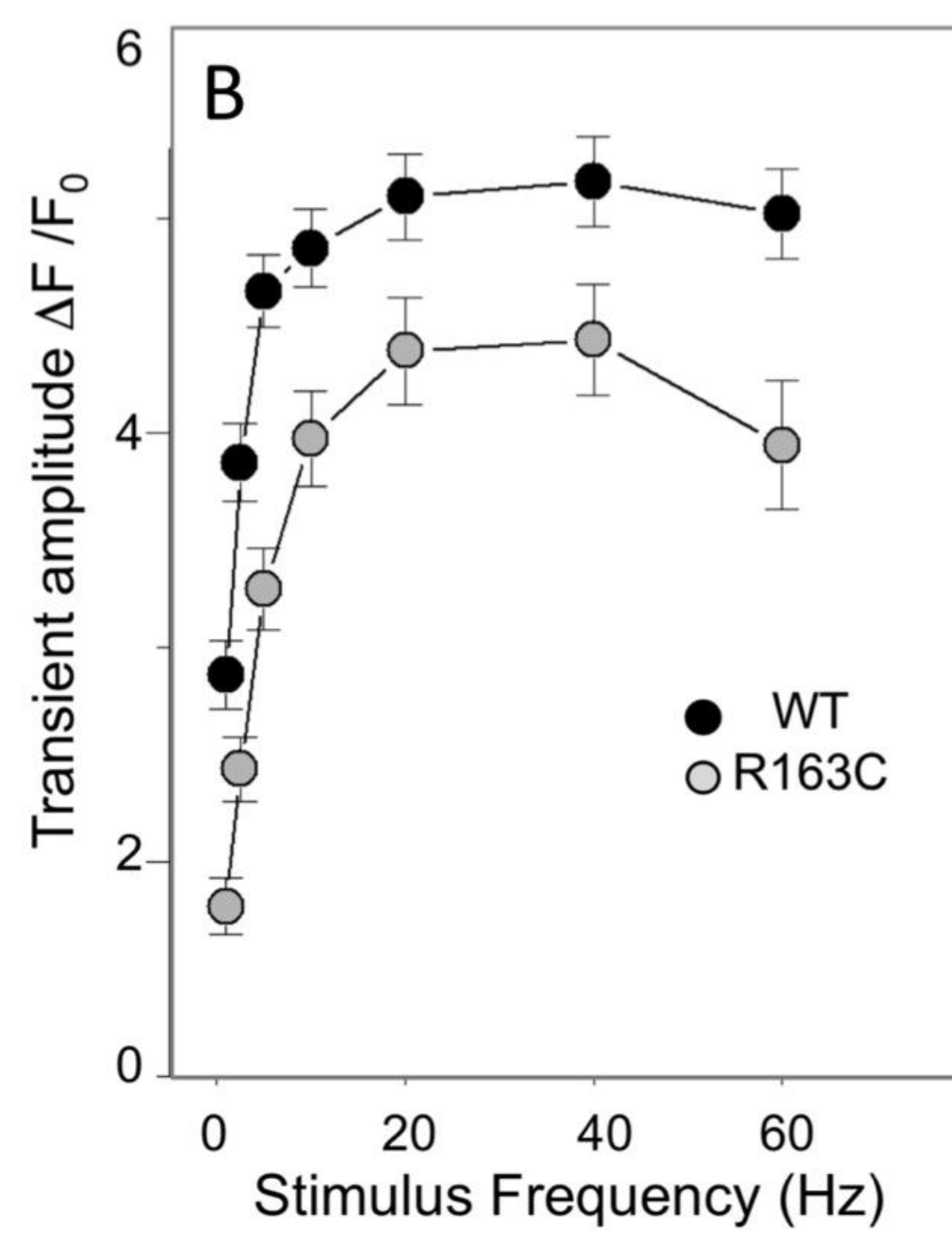
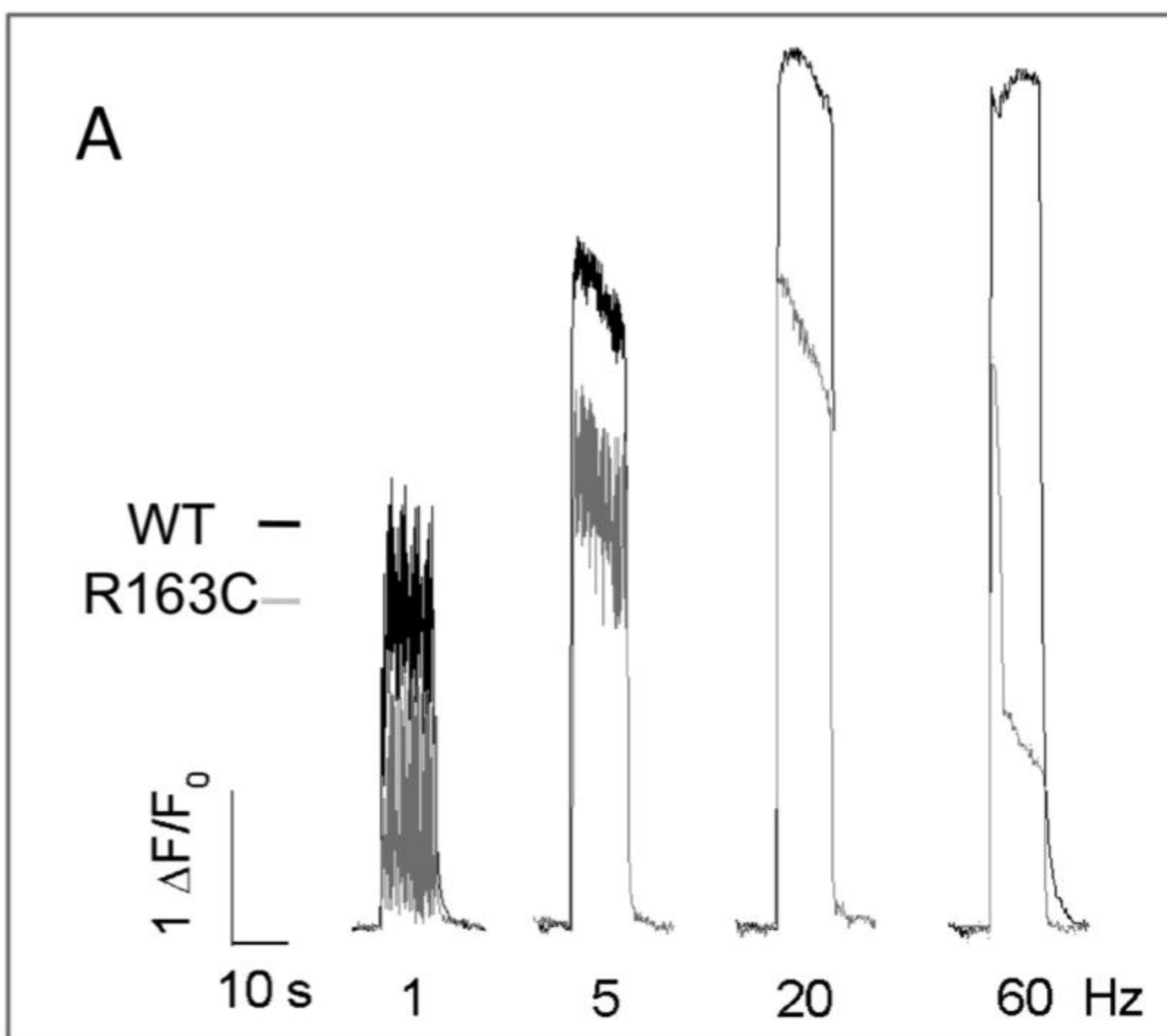


Figure 1

Adult FDB Fibers

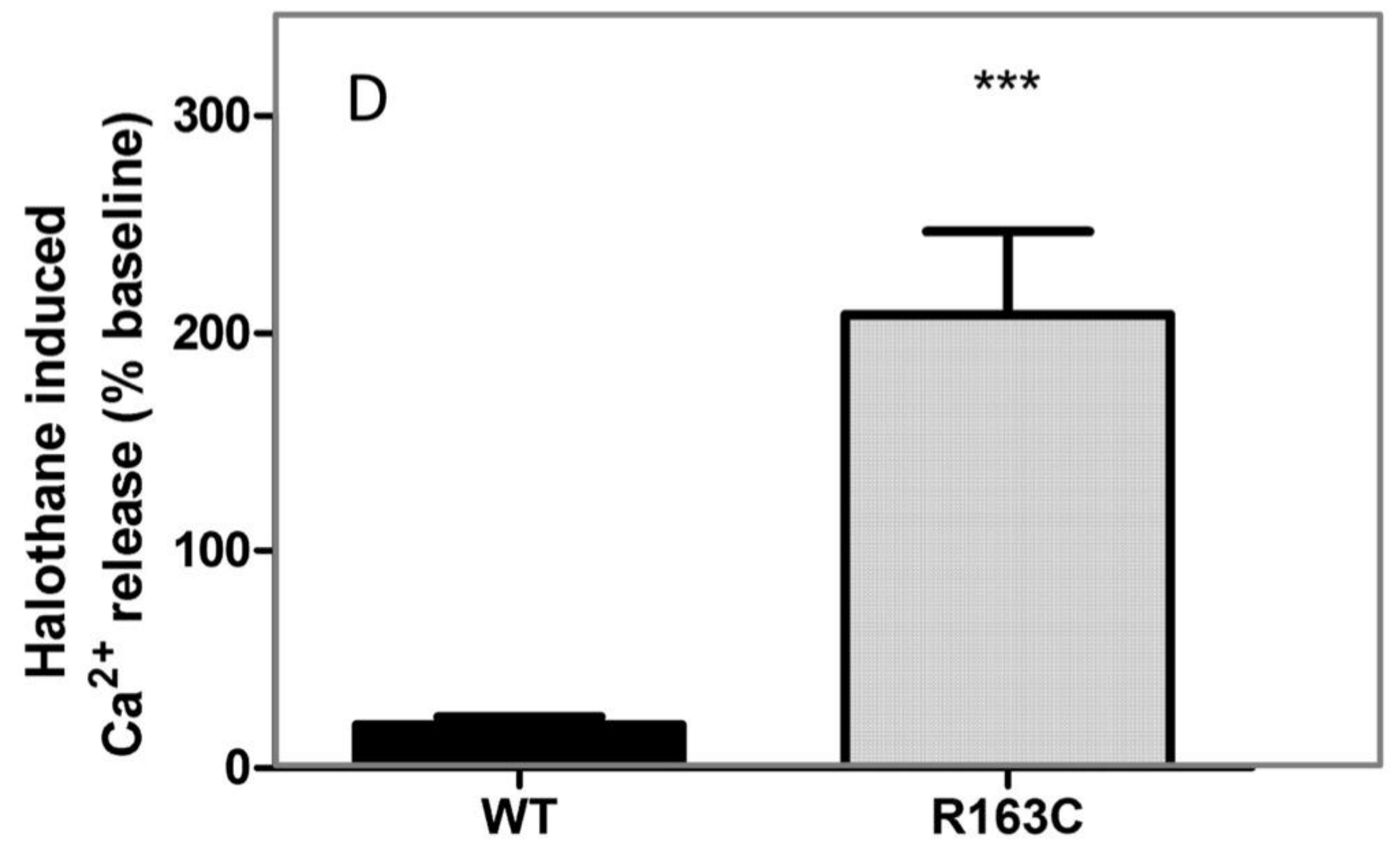
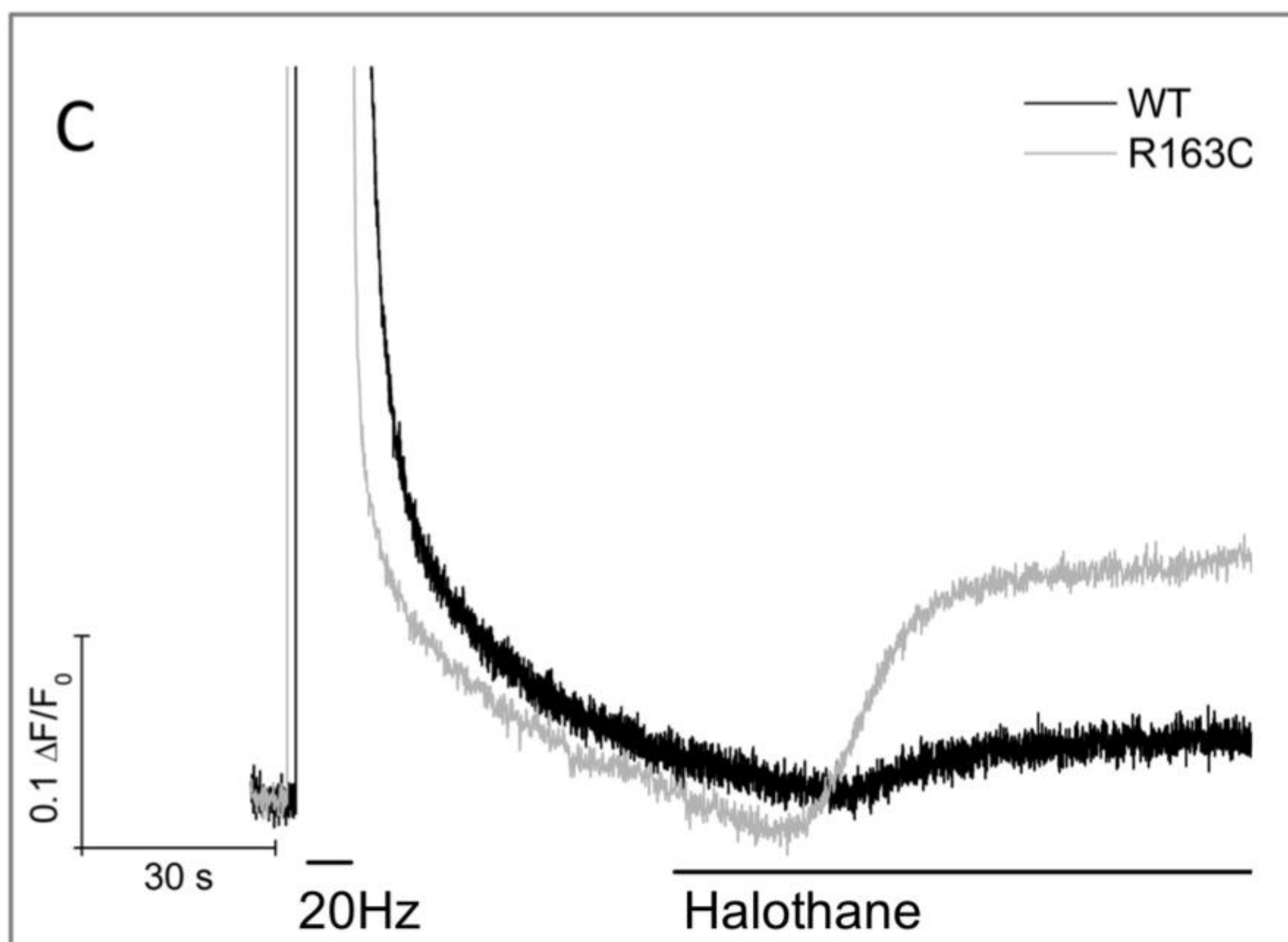
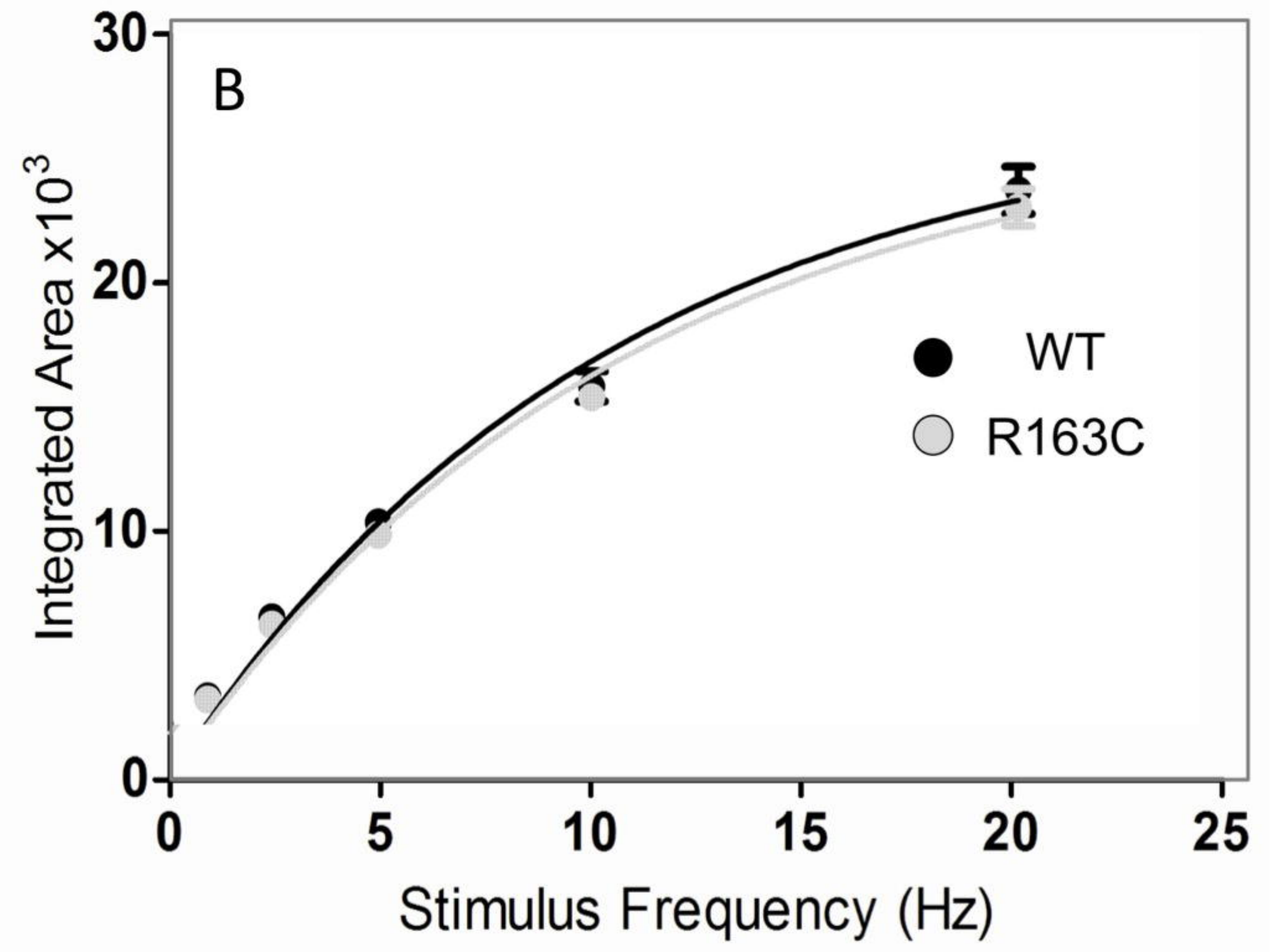
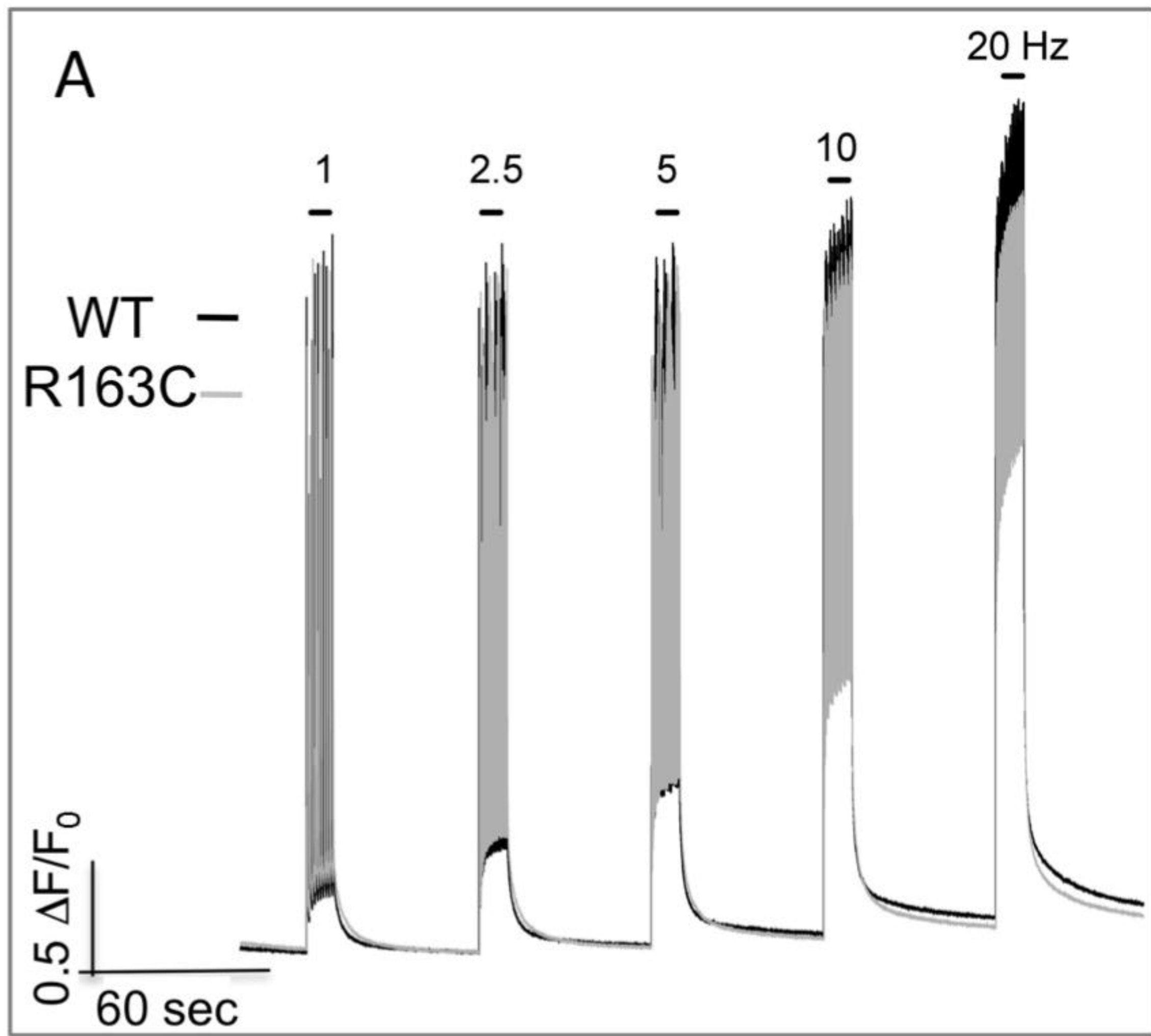
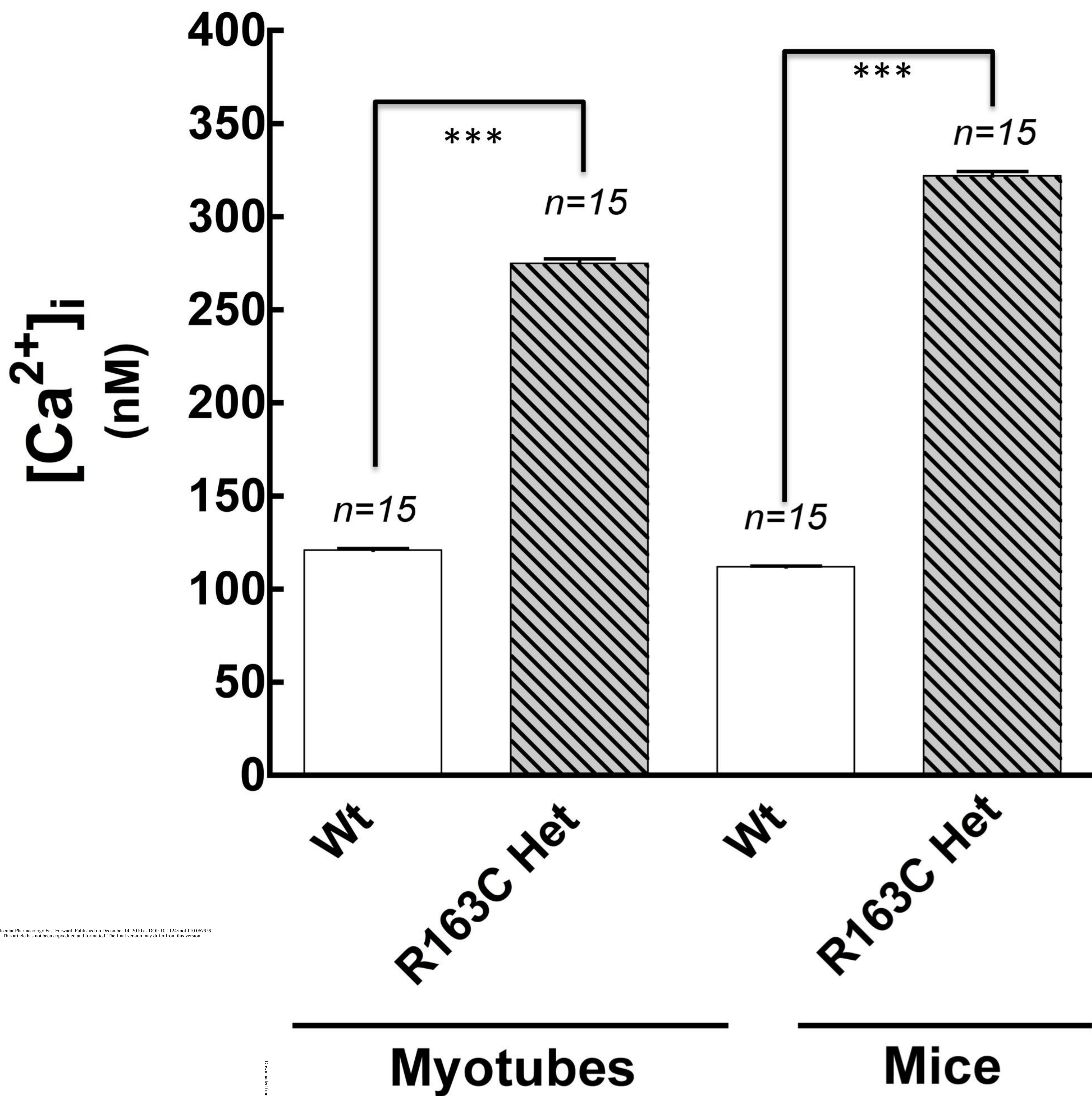


Figure 2

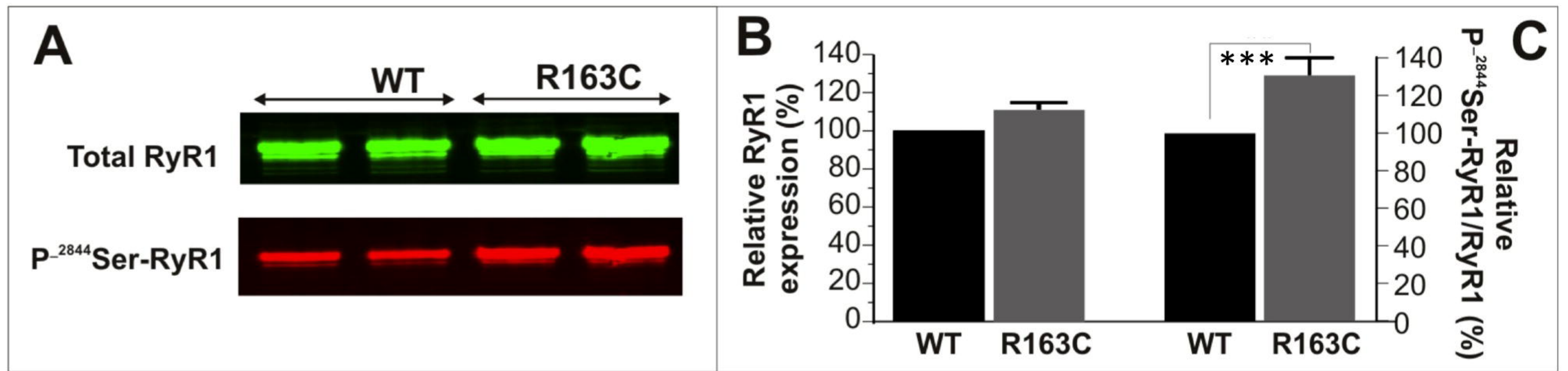


Molecular Pharmacology Fast Forward. Published on December 14, 2010 as DOI: 10.1124/mol.110.067999
 This article has not been certified for copyright and format. The final version may differ from this version.

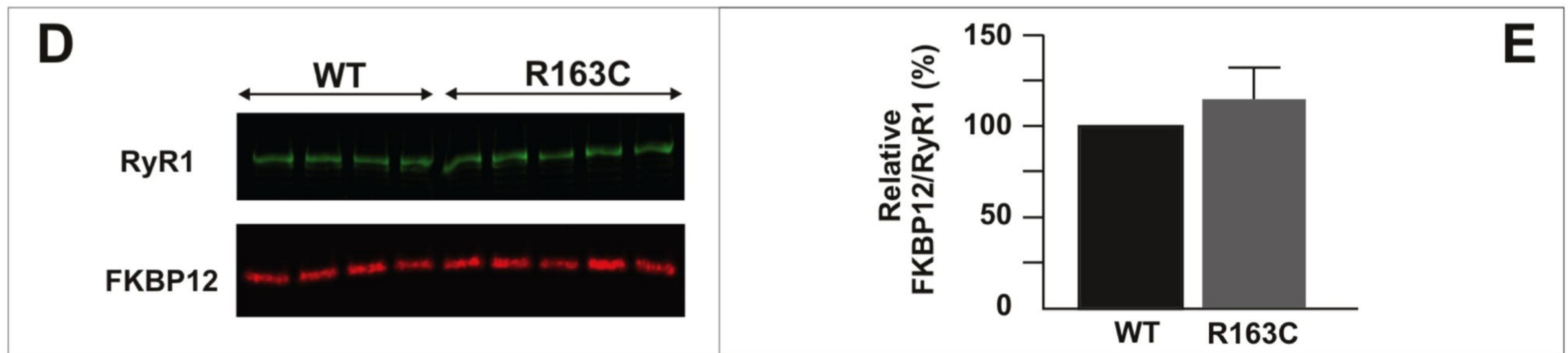
Downloaded from molpharm.physocpubs.org at ASHET Journals on April 19, 2024

Figure 3

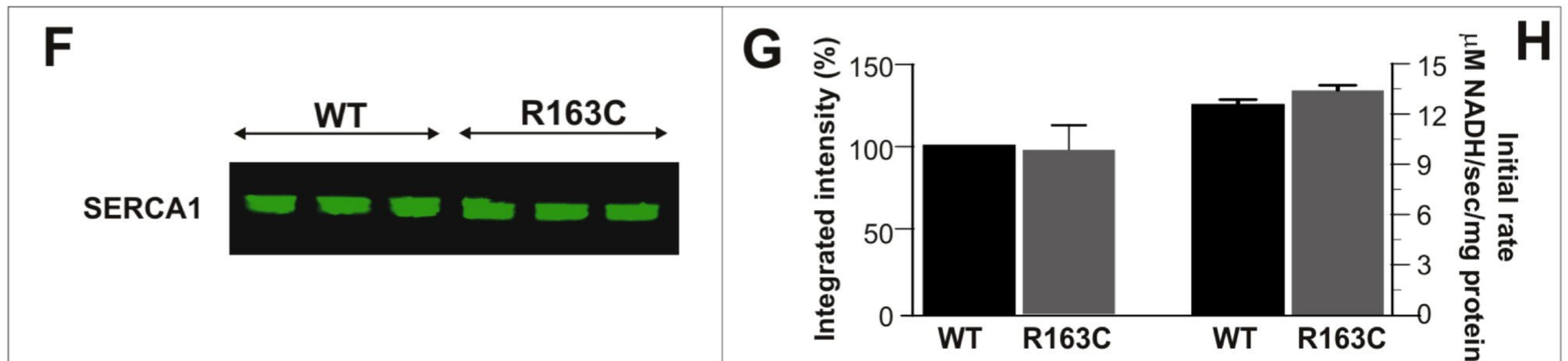
RyR Expression and Phosphorylation

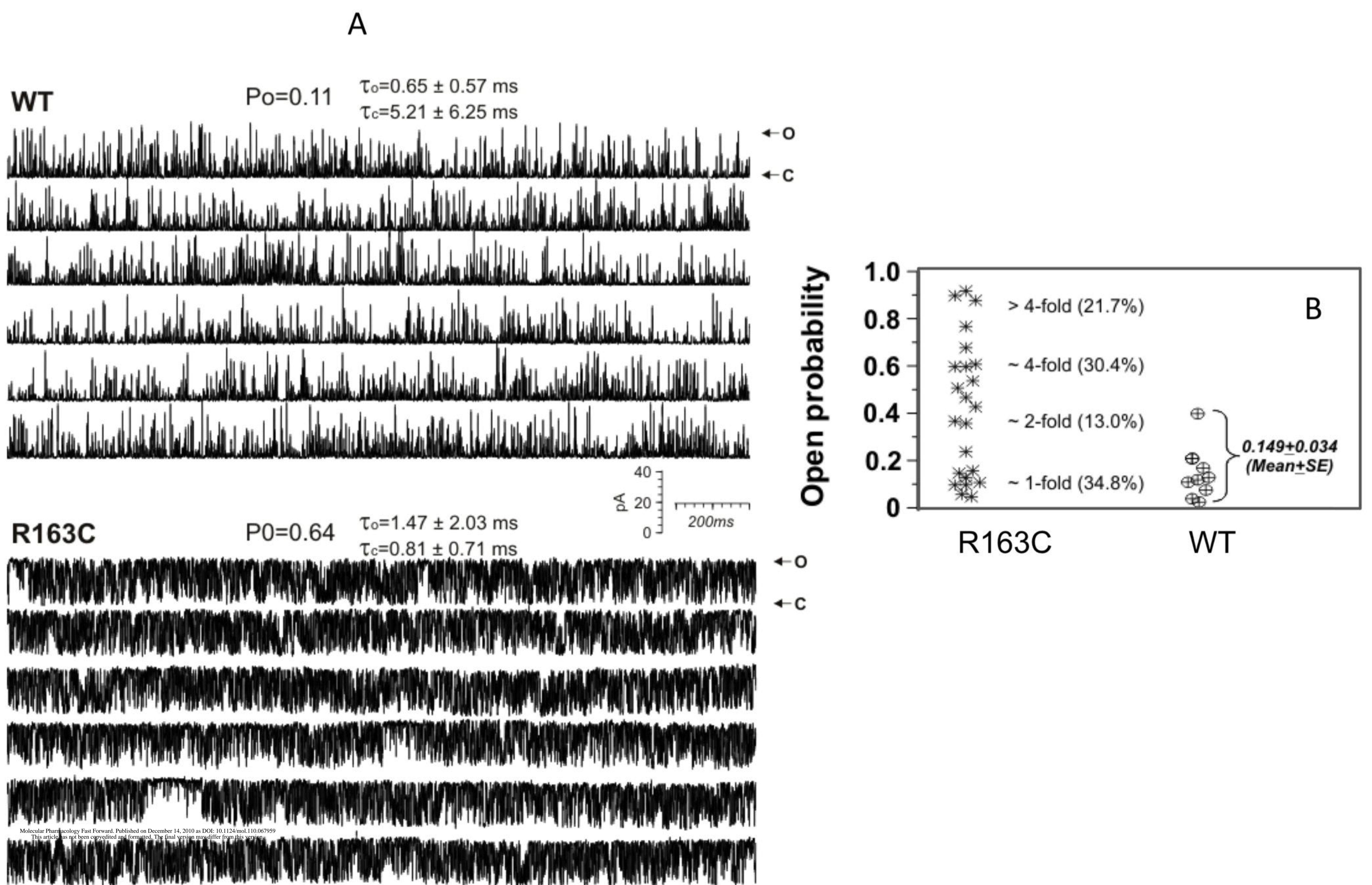


FKBP12 Expression



SERCA1 Expression and Activity

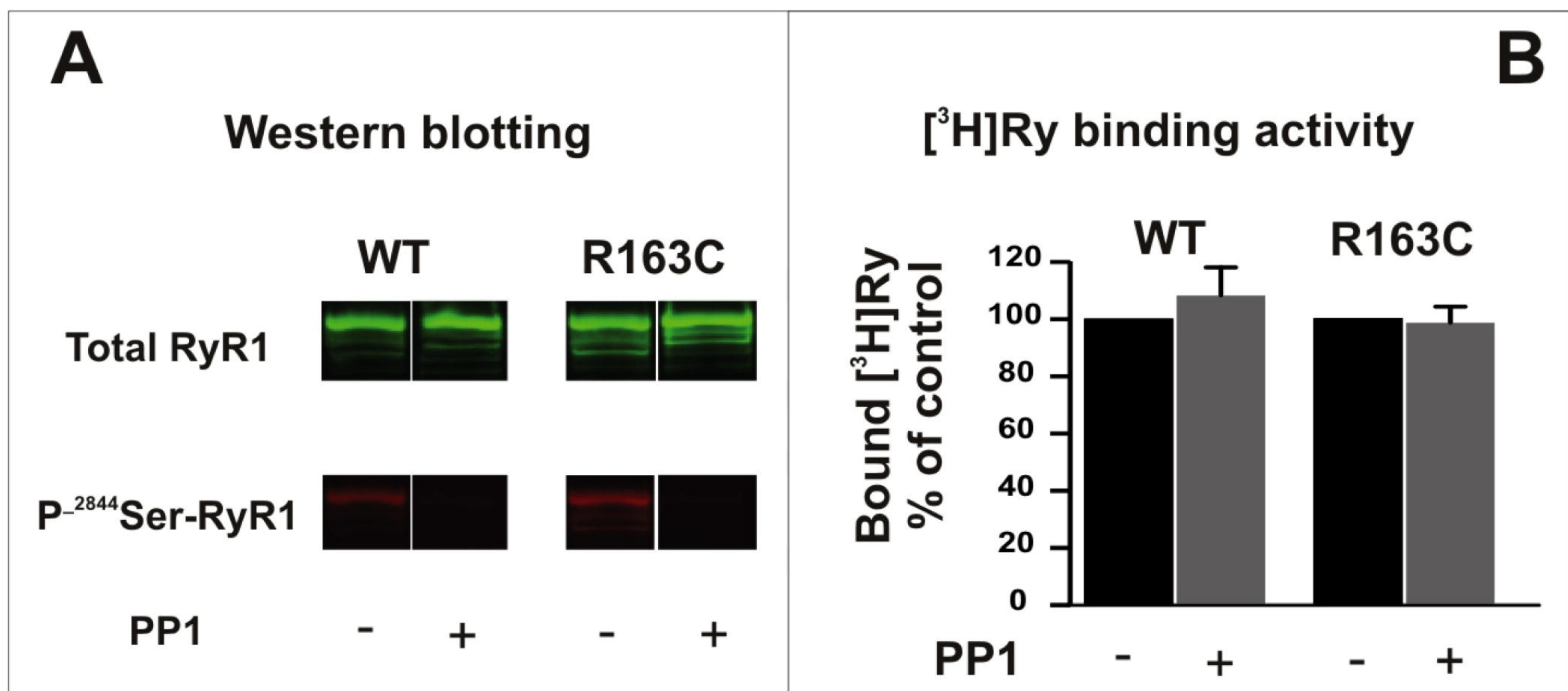


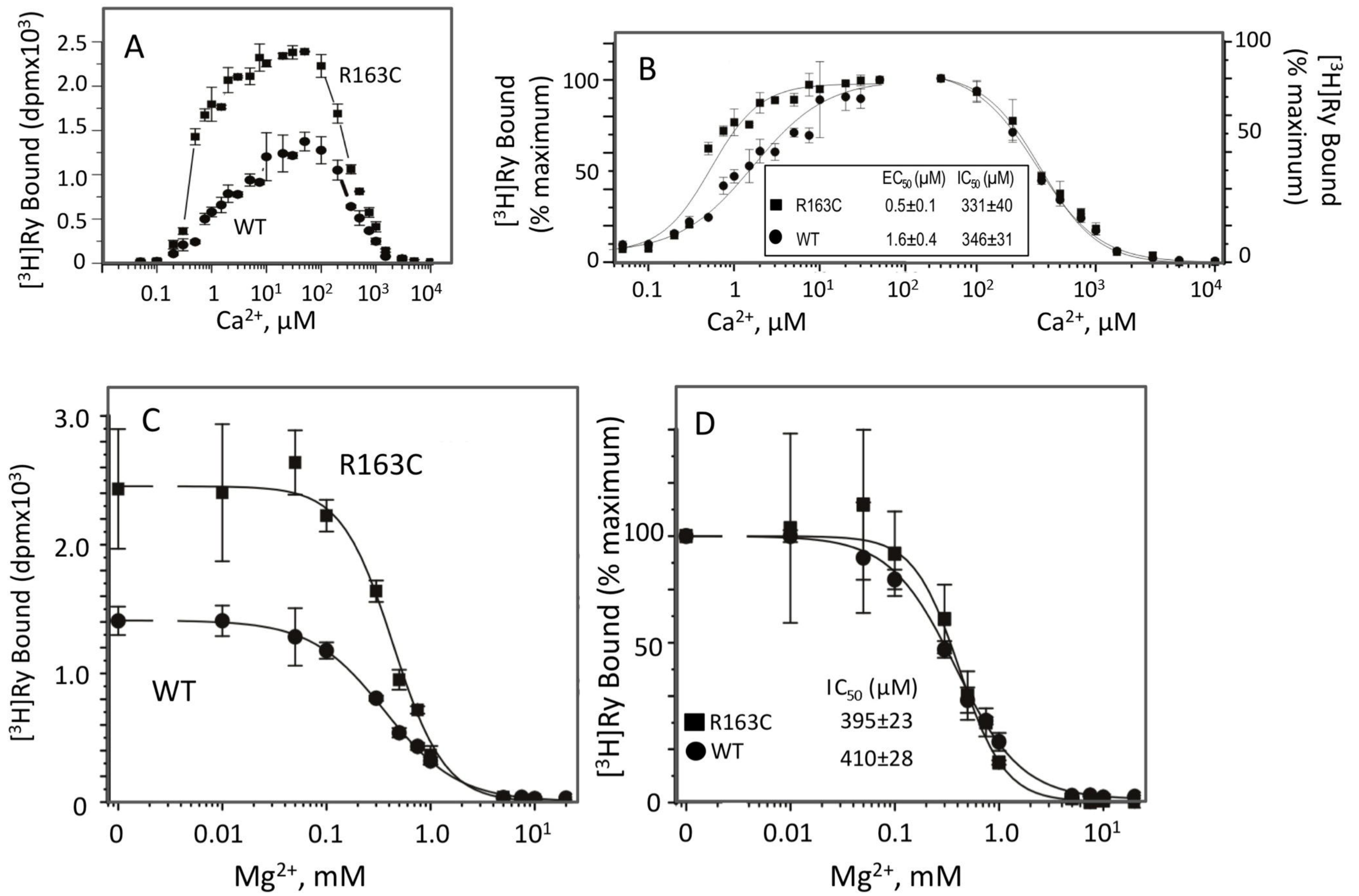


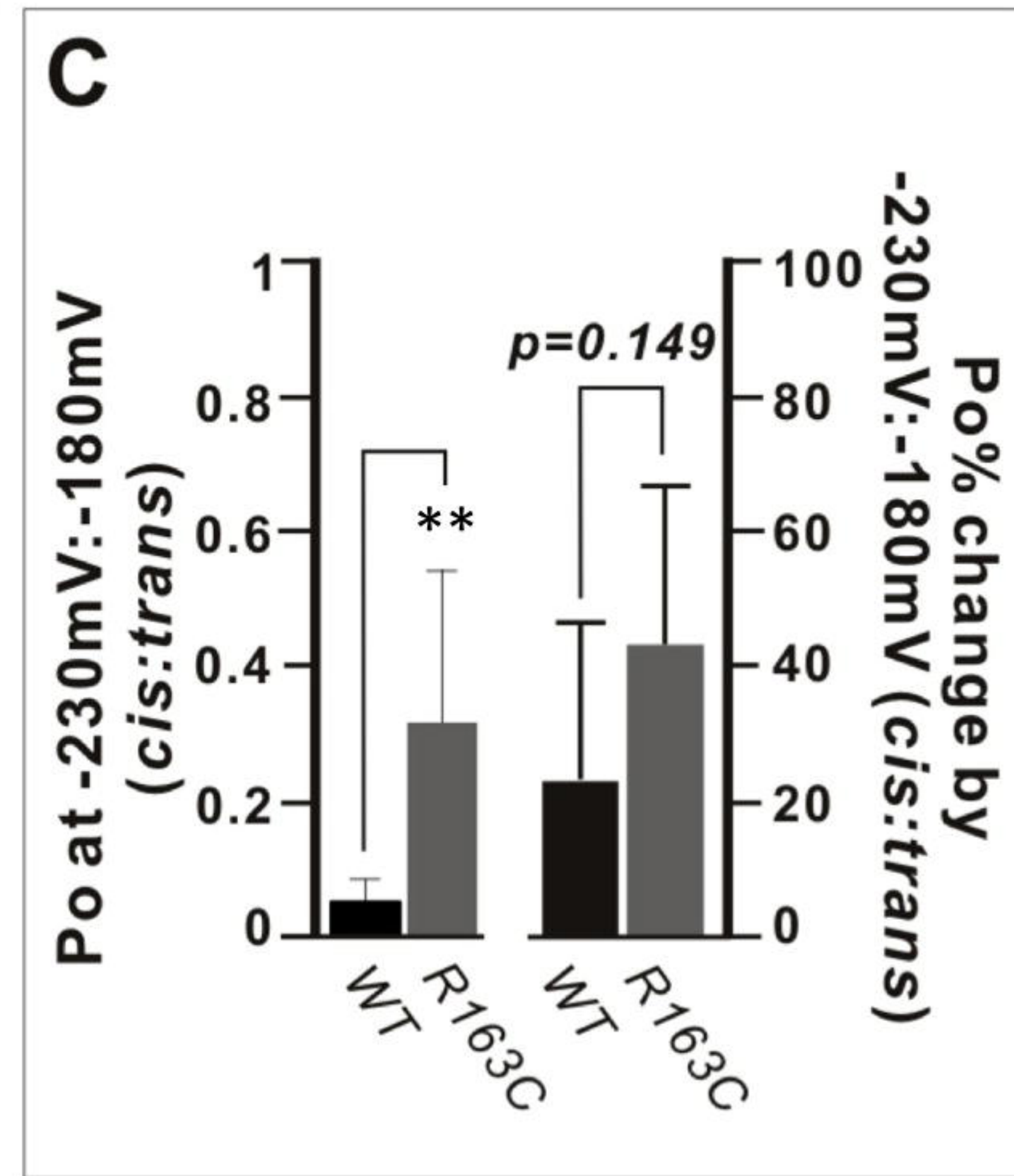
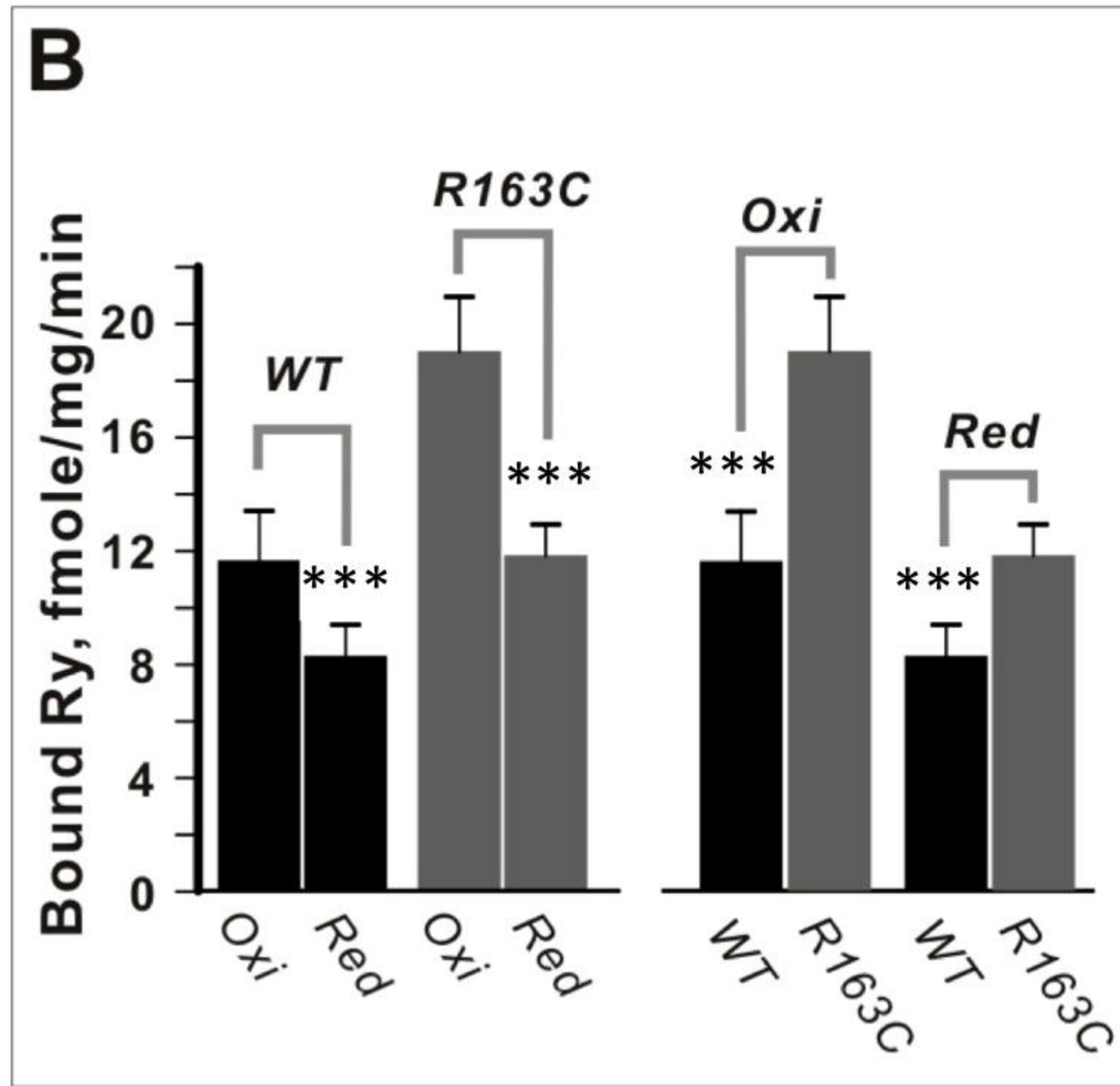
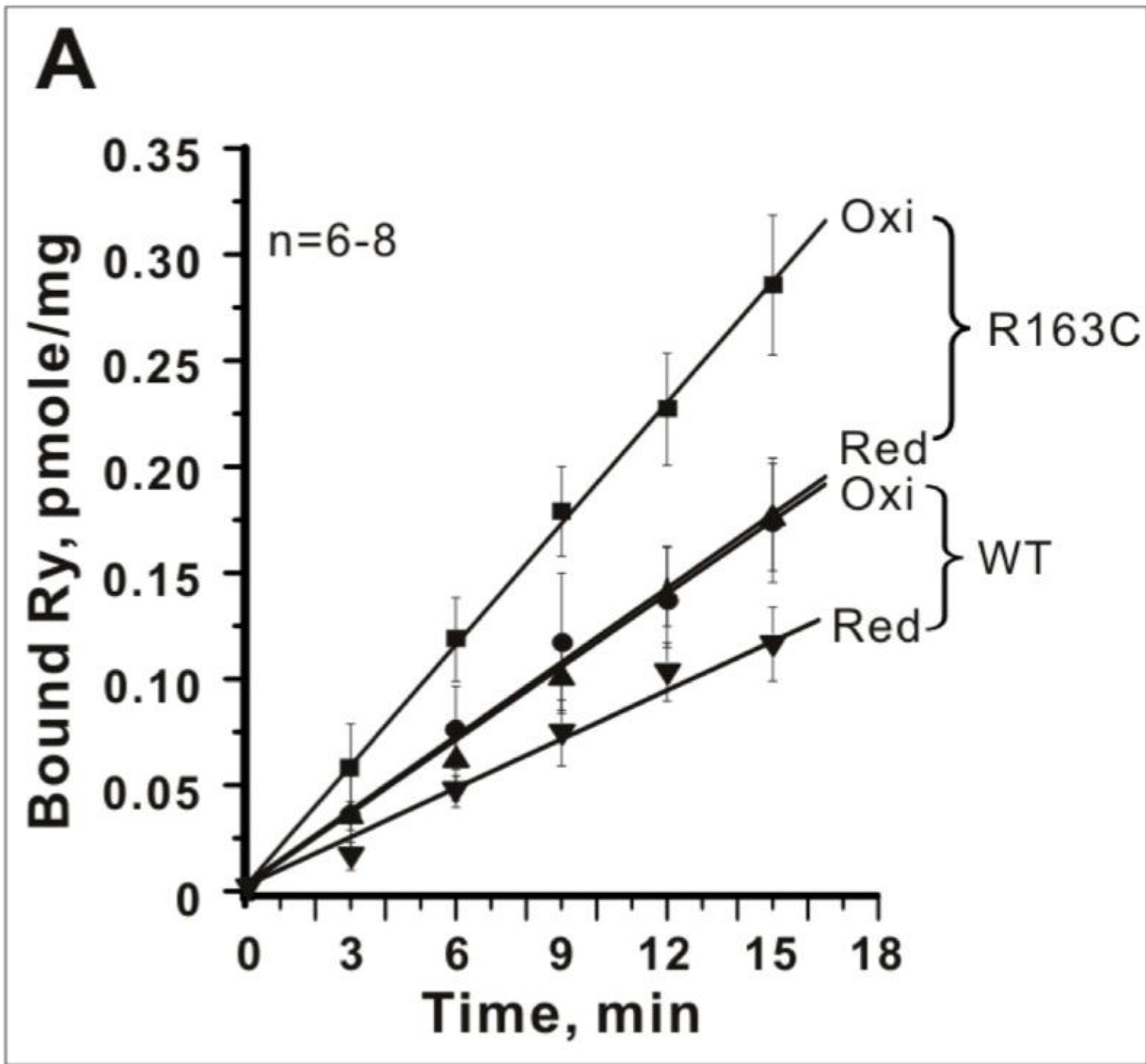
Molecular Pharmacology Fast Forward. Published on December 14, 2010 as DOI: 10.1124/mol.110.067959
This article has not been certified for peer review. The copyright owner for this article is the American Society for Pharmacology and Experimental Therapeutics.

Downloaded from molpharm.aphpharmsoc.org at ASHPT Journals on April 19, 2024

Figure 5







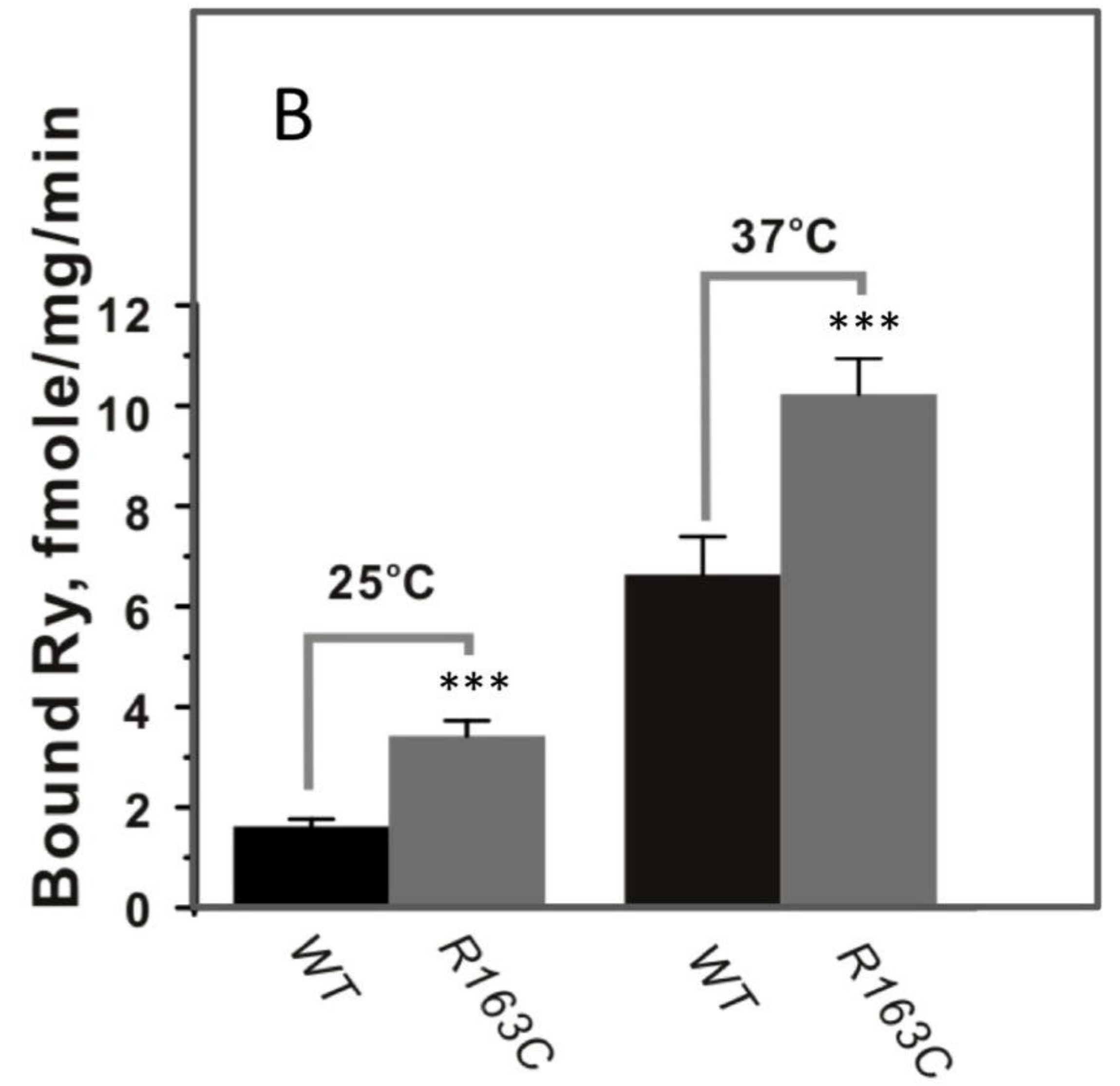
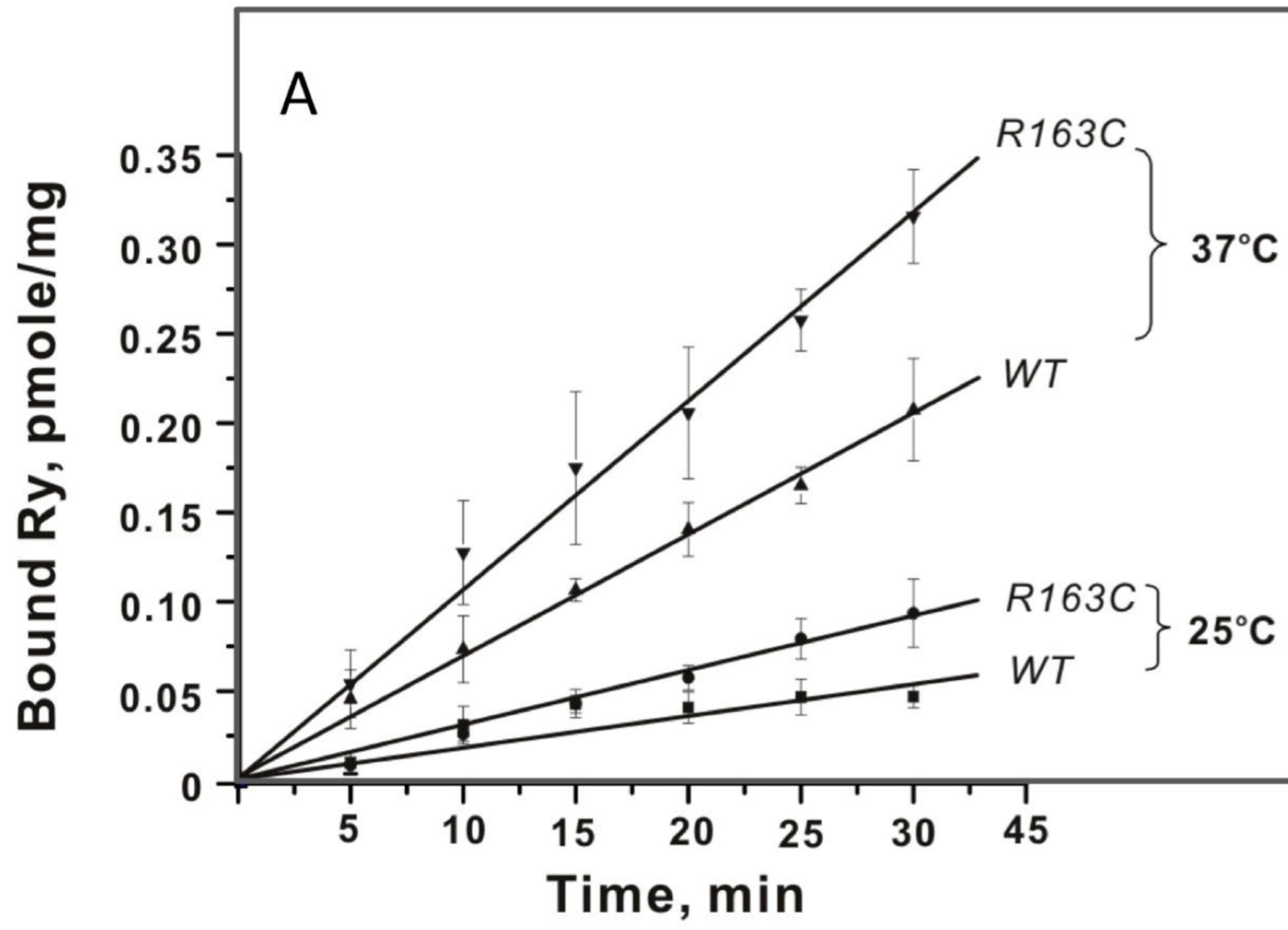


Figure 9